AD-A125 830 AUTOMATIC SCALING OF DIGISONDE IONOGRAMS TEST AND EVALUATION REPORT(U) LOWELL UNIV RESEARCH FOUNDATION MA B W REINISCH ET AL. SEP 82 ULRF-421/CAR AFGL-TR-82-0324 1/1

UNCLASSIFIED F19628-80-C-0064 F/G 12/1 NL

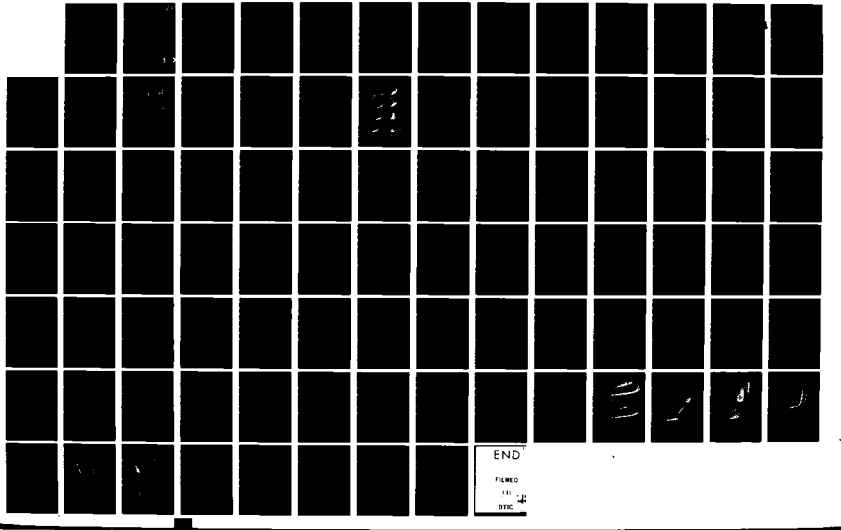

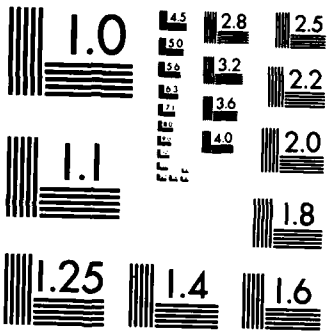

AFGL-TR-82-0324

AUTOMATIC SCALING OF DIGISONDE IONOGRAMS TEST AND EVALUATION REPORT

Bodo W. Reinisch
Jane S. Tang
Robert R. Gamache

University of Lowell
Center for Atmospheric Research
450 Aiken Street
Lowell, Massachusetts 01854

September 1982

Scientific Report No. 4

AIR FORCE GEOPHYSICS LABORATORY
AIR FORCE SYSTEMS COMMAND
UNITED STATES AIR FORCE
HANSCOM AFB, MASSACHUSETTS 01731

UNCLASSIFIED

SECURITY CLASSIFICATION OF THIS PAGE (When Data Entered)

REPORT DOCUMENTATION PAGE	READ INSTRUCTIONS BEFORE COMPLETING FORM
1. REPORT NUMBER: AFGL-TR-82-0324	2. GOVT ACCESSION NO.: AD-A125830
	3. RECIPIENT'S CATALOG NUMBER:
4. TITLE (and Subtitle): AUTOMATIC SCALING OF DIGISONDE IONOGRAMS TEST AND EVALUATION REPORT	5. TYPE OF REPORT & PERIOD COVERED: Scientific Report No. 4 1 Oct 1981-30 Sep 1982
	6. PERFORMING ORG. REPORT NUMBER: ULRF-421/CAR
7. AUTHOR(s): Bodo W. Reinisch, Jane S. Tang, Robert R. Gamache	8. CONTRACT OR GRANT NUMBER(s): F19628-80-C-0064
9. PERFORMING ORGANIZATION NAME AND ADDRESS: University of Lowell, Center for Atmospheric Research, 450 Aiken Street, Lowell, Massachusetts 01854	10. PROGRAM ELEMENT, PROJECT, TASK AREA & WORK UNIT NUMBERS: 62101F; 464306AJ
11. CONTROLLING OFFICE NAME AND ADDRESS: Air Force Geophysics Laboratory, Hanscom AFB, Massachusetts 01731, Contract Monitor: J. Waaramaa/PHY	12. REPORT DATE: September 1982
	13. NUMBER OF PAGES: 90
14. MONITORING AGENCY NAME & ADDRESS (if different from Controlling Office)	15. SECURITY CLASS. (of this report): Unclassified
	15a. DECLASSIFICATION/DOWNGRADING SCHEDULE

16. DISTRIBUTION STATEMENT (of this Report)

Approved for public release; distribution unlimited.

17. DISTRIBUTION STATEMENT (of the abstract entered in Block 20, if different from Report)

18. SUPPLEMENTARY NOTES

19. KEY WORDS (Continue on reverse side if necessary and identify by block number)

Automatic Scaling
Digital Ionograms
Ionogram Scaling
Electron Density Profiles
Real Time Profiles
Ionogram Parameters

20. ABSTRACT (Continue on reverse side if necessary and identify by block number)

Some 8000 Digisonde ionograms from a subauroral station, Goose Bay, Labrador, were automatically scaled. The h'(f) traces together with all important ionospheric parameters are determined: critical frequencies, minimum frequencies, heights, spread, amplitude and Doppler frequencies. The electron density profiles are calculated using the profile-fitting method developed at the University of Lowell. For four months

DD FORM 1 JAN 73 1473 EDITION OF 1 NOV 65 IS OBSOLETE

UNCLASSIFIED

SECURITY CLASSIFICATION OF THIS PAGE (When Data Entered)

20. Abstract

in 1980, January, April, July and September, the hourly ionogram parameters are compared with the values obtained by manually scaling the ionograms. For a data base of 2226 ionograms 95% were scaled within an foF2 error of 1 MHz, and 90% within 0.5 MHz. The MUF(3000) was determined within 10% for 88% of the ionograms. Approximately 50% of all ionograms show spread F.

TABLE OF CONTENTS

LIST OF FIGURES

LIST OF FIGURES (Continued)

LIST OF FIGURES (Continued)

LIST OF TABLES

1.0 INTRODUCTION

Ionograms contain as basic information the virtual range versus frequency. The Digisonde 128PS [Bibl and Reinisch, 1978] also measures amplitude, phase, polarization, incidence angle and the spectral signature of the echoes. This allows automatic scaling of the ionograms and conversion to vertical electron density profiles. This report discusses the automatic scaling of some 8000 Digisonde ionograms from the Goose Bay Ionospheric Observatory (64.6N geomagnetic) of the Air Force Geophysics Laboratory. These ionograms display a large variety of features: quiet and disturbed daytime recordings, heavy spread F during the night, the mid-latitude trough moving over the station, fast variation of the ionospheric parameters and frequent absorption events.

Sections 2, 3 and 4 give a brief description of the data base and the automatic scaling methods that extract the required ionospheric parameters from the digital ionograms. A few examples illustrate the results of the profile-fitting method that is used to calculate the electron density profiles from the autoscaled echo traces. It is the first time that anybody has succeeded to automatically scale a large number of quiet and disturbed ionograms. To establish a level of confidence in the scaling algorithm, the critical frequency and height values for more than 2000 hourly ionograms of January, April, July and September 1980 were compared with the manually scaled values. Section 5 shows that for 90% of all ionograms the error in foF2 is less than 0.5 MHz; the rate is 95% for a 1 MHz error limit. This is an excellent result considering the subauroral location of Goose Bay. The Automatic Real Time Ionogram Scaler with True Height Calculation (ARTIST) which is based on the 8086 microprocessor is briefly described in Section 6.

2.0 DATA BASE

The routine ionograms at the Goose Bay Ionospheric Observatory (53.3N, 60.5W geographic, 64.6N, 12.1W geomagnetic) measure and record amplitude, polarization, incidence angle and Doppler frequency as a function of frequency and range. The lower part of Figure 1 shows a quiet amplitude ionogram containing all signals. Removal of the non-vertical and X-polarization signals results in the upper ionogram of Figure 1, which is much easier to scale automatically. The X-trace data are not discarded; they are used for the accurate determination of foF2. For bottomside ionograms, the O-trace is generally better presented than the X-trace and our autoscaling effort concentrated therefore on the O-trace. This is in contrast to topside ionograms where O and X-polarization echoes dominate alternatingly [Reinisch and Huang, 1982].

Four months of tape recorded ionograms for January, April, July and September 1980 were processed to test for any seasonal dependence of the scaling accuracy. Three vertical ionograms were recorded per hour, except in September when 6 ionograms per hour were stored. Disregarding any of the technically incomplete ionograms, about 8000 ionograms were autoscaled. The parameters of 2226 hourly ionograms were compared with the manually scaled values.

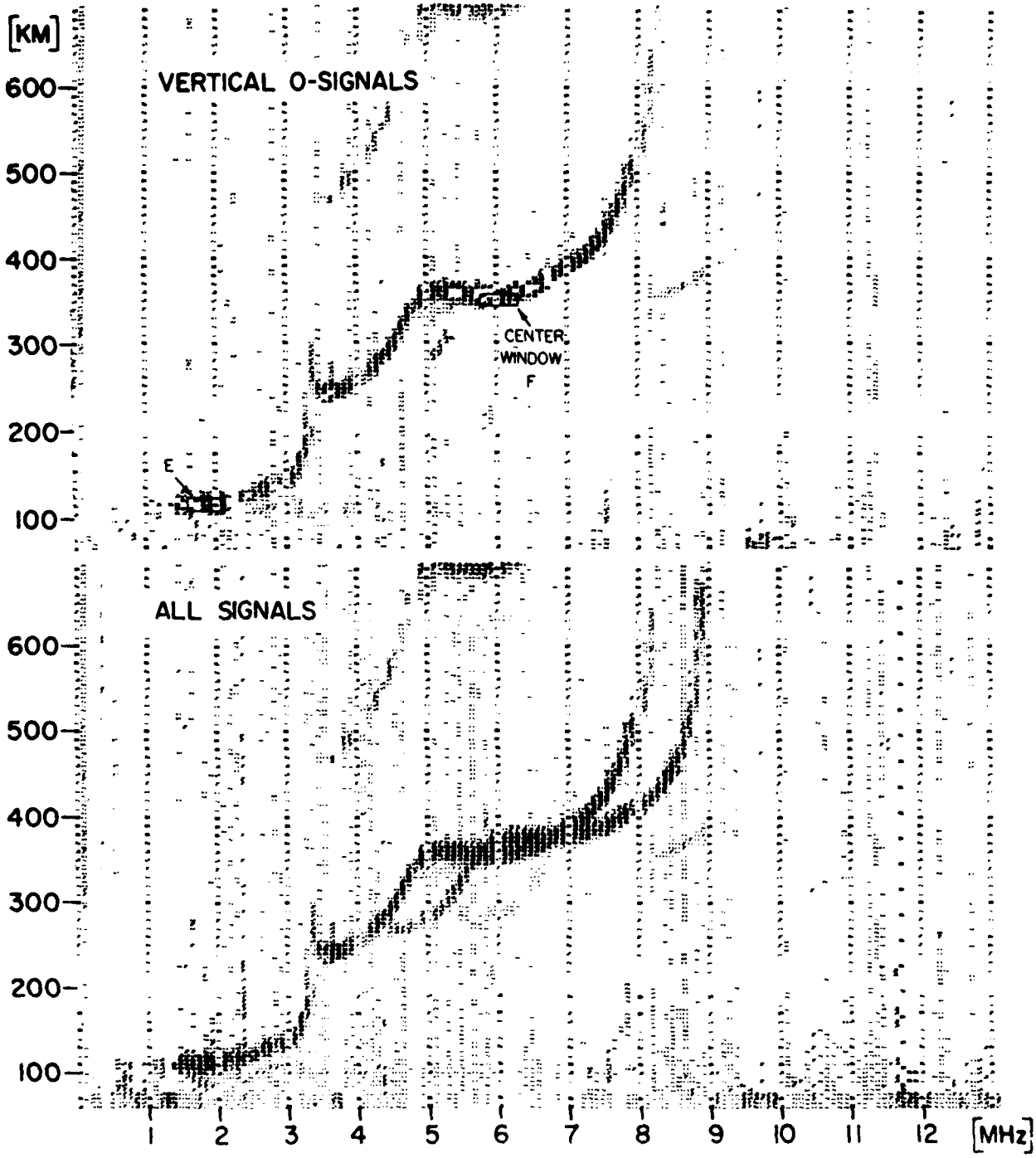

UNDISTURBED DAY IONOGRAM
GOOSE BAY 16 JUN 1980 17:20 AST

Figure 1

3.0 SCALING ALGORITHM

The ideas and procedures for the automatic scaling of digital ionograms have been published in a series of papers [Reinisch and Huang, 1982; Huang and Reinisch, 1982; Reinisch, Moses and Tang, 1981]. A paper on the processing of bottomside Digisonde ionograms has been submitted for publication to Radio Science. Appendix A is a preprint of this paper, describing in detail the scaling algorithms and the profile-fitting method developed for the calculation of the electron density profile. It suffices to give here a brief summary.

Ideal ionograms, recorded under quiet conditions with a relatively low level of interference, pose no difficulties for automatic scaling, yet they are useful to illustrate some of the scaling procedures. (Manufacturers of ionosondes generally select such quiet ionograms to demonstrate system performance and the capability of automatic scaling. We refer to Figures 3, 4 and 7 in Appendix A for examples of disturbed ionograms which are successfully scaled by the ULCAR algorithm.) It is important to emphasize that even at mid-latitude the percentage of unusual or disturbed ionograms might be as high as 30%. The basic concepts of the scaling procedure must take into account this fact. In general, the vertical O and X echo traces must be found within spread F signals. Multiples and oblique echoes must be eliminated relying on the amplitude, polarization and incidence angle information contained in the Digisonde ionograms. This is only possible by examining the ionogram in its entirety.

To find the F trace the ionogram is surveyed for heights larger than 160 km, and the "center window" (Figure 1) with the maximum signal energy is determined. A first approximate trace, the baseline, is constructed by sliding a searching window toward higher and lower frequencies. Two hyperbolic functions

$$h'_X = r + \frac{1}{a+bf}$$

and

$$h'_O = r + \frac{1}{a+b[f+\frac{1}{2}fH]}$$

are fitted to the O and X amplitude pixels in order to determine foF2, the critical frequency of the F2 layer; f and fH are sounder and gyrofrequency, respectively. The block diagram in Figure 2 gives an outline of the F-trace extraction.

The main difficulties for the E-region are the identification of E, Es and night E. To find the normal E trace an analytic function is fitted to the amplitude pixels. The function is derived from a parabolic profile and the three parameters of the parabola, height, half width and peak density, are determined such as to maximize the average signal amplitude of the ordinary vertical echoes traced out by the h'(f) function. Continuous O echoes beyond foE are identified as Es trace. To save CPU time, the search for the peak density (or foE) of the parabolic E-layer is limited to ±0.3 MHz around a predicted mean value. For evening and night times the search is extended to 6 MHz, an empirical upper limit for night E critical frequencies.

BLOCK DIAGRAM FOR THE EXTRACTION OF THE F-TRACE

ULCAR
OCT 82

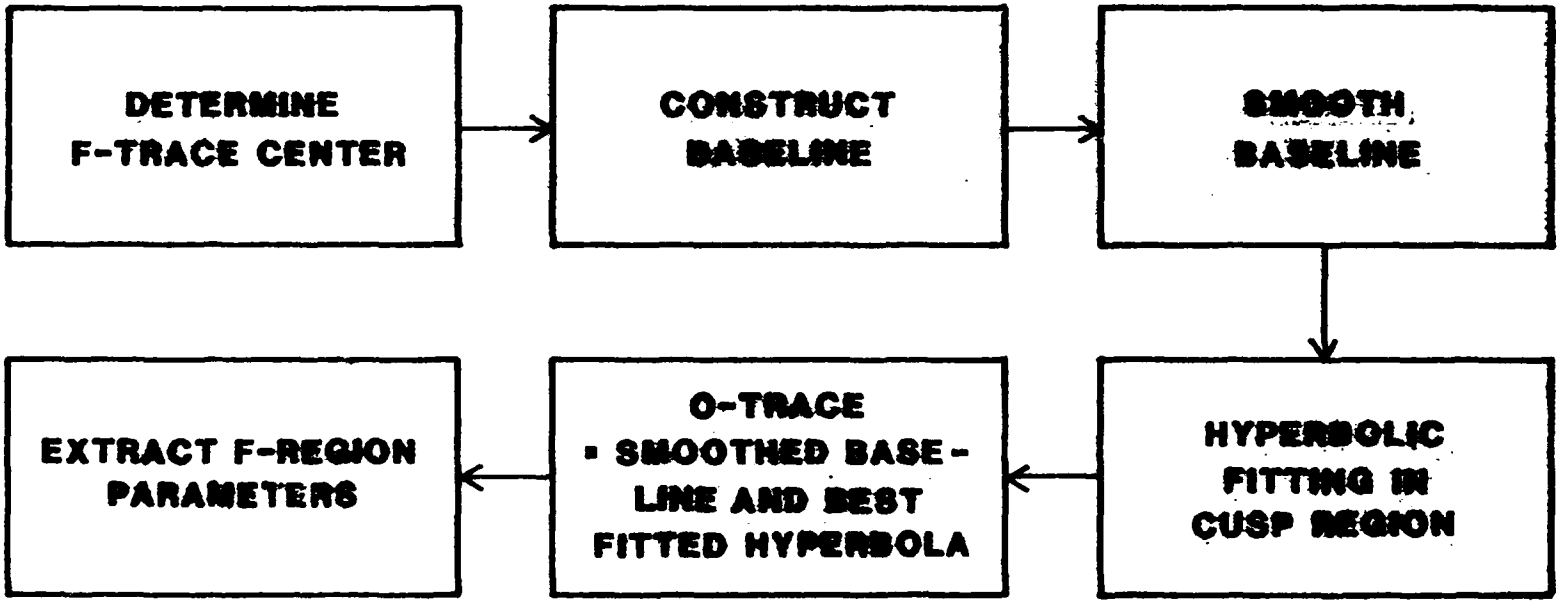

Figure 2

4.0 SCALED PARAMETERS AND ELECTRON DENSITY PROFILES

Once the E and F region traces $h'(f_i)$ are focused, the program determines the following parameters.

(1)	foF2	F2 layer critical frequency
(2)	foF1	F1 layer critical frequency
(3)	MUF(3000)	Maximum usable frequency for D = 3000 km
(4)	M(3000)	MUF (3000)/foF2
(5)	fminF	Minimum frequency for F echoes
(6)	fmin	Minimum frequency for E or F echoes
(7)	foE	E layer critical frequency
(8)	foEs	Es layer critical frequency
(9)	h'F	Minimum virtual height of F trace
(10)	h'F2	Minimum virtual height of F2 trace
(11)	h'E	Minimum virtual height of E trace
(12)	h'Es	Minimum virtual height of Es trace

The scaling accuracy of parameters (1) to (12) is statistically evaluated in Section 5. The following parameters are also determined, but no evaluation is given in this report.

(13)	FQ	Average range spread of F echoes
(14)	fXI	Maximum frequency of F trace; fXI-fXF2=F region frequency spread
(15)	EQ	Average range spread of E echoes
(16)	fminE	Minimum frequency of E echoes
(17)	A	Echo amplitudes, normalized to 100 km reflection height, for each MHz
(18)	Vz	Vertical velocity deduced from doppler measurements

All these parameters are available as program output together with the $h'(f_i)$ array.

Having $h'(f_i)$ available it is of course possible to calculate the electron density profile [for example, Doupnik and Schmerling, 1965]. Since the autoscaling method produces some occasional wild points which are likely to adversely effect the conventional lamination procedure we developed the profile-fitting technique for the calculation of the F-region profile. The F-profile is represented by a single analytical function consisting of a modified sum of shifted Chebyshev polynomials [Huang and Reinisch, 1982, p. 838, eq. 6]. The idea of polynomial fitting had been suggested earlier [Titheridge, 1967]. A parabolic approximation of the E-region profile is automatically obtained in the E layer scaling routine. E and F profiles are joining smoothly allowing for a parabolic valley (see Figure 9 in Appendix A) between the E and F region. Comparisons between manual and autoprofiles are given in Figures 10, 11 and 12 in Appendix A.

5.0 PERFORMANCE EVALUATION OF THE IONOGRAM SCALING ALGORITHM

It is always easy to automatically scale a few selected ionograms by tailoring the scaling algorithms to these specific ionograms. The real test is the application of the algorithm to a large number of ionograms covering day, night and twilight as well as quiet and disturbed conditions. To test the performance of the BISA (Bottomside Ionogram Scaling Algorithm) program, more than 8000 ionograms for January, April, July and September 1980 from Goose Bay, Labrador, were processed. This data base is representative of one year's data covering all seasons and all types of ionospheric conditions. The parameters of the approximately 2200 hourly ionograms were compared with the manually scaled values.

The difficulty of the scaling task is illustrated by the sequence of ionograms in Figure 3 recorded in Goose Bay on 7 January 1980 between 1819 and 2039 AST. It is the time when the F-region trough moves over the station causing spread F and oblique echoes. The preliminary results of the autoscaling, indicated by the small filled circles, are in good agreement with manual interpretation. (The final h'(f) traces are obtained by lowering the preliminary traces to best fit the leading edge of the pulse.) The amplitude ionograms in Figure 3 contain the O and X-echoes as well as oblique returns. If reflections from the trough walls or other irregularities, like at 1959 AST, produce several retardation cusps in the ionogram, the program selects the vertical O-echo sequence with the strongest amplitudes. A manual evaluator may scale foF2 at 1959 AST as 2.7 or 3.2 MHz, while the program scaled 4.3 MHz and jumped to the lower value at 2019 AST. These differences in "interpretation" are the main contributor to errors in foF2 above 0.5 MHz.

5.1 Comparing Manual with Autoscaling Results

The parameters obtained from the BISA program are compared to the corresponding manually scaled parameters to test the accuracy

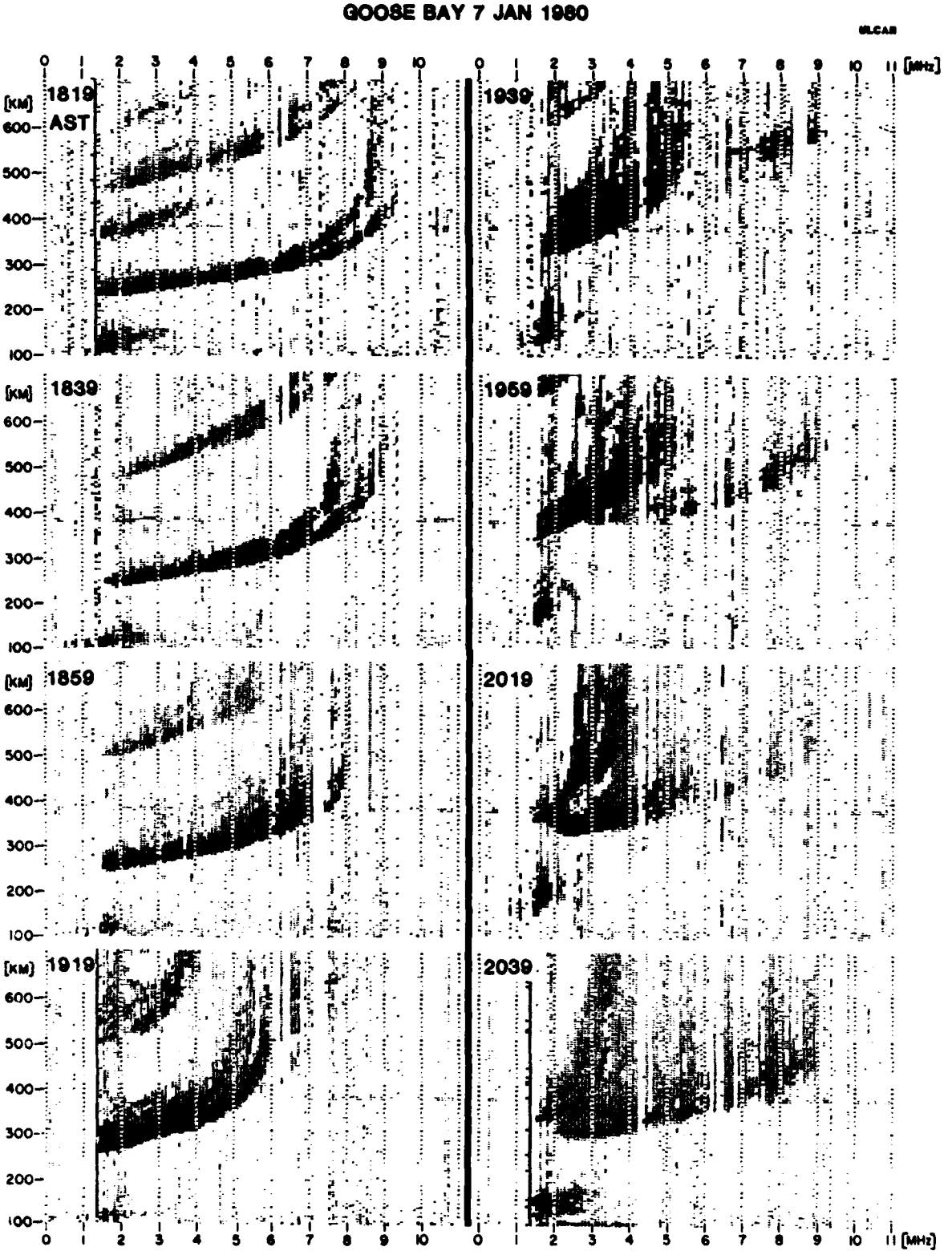

AUTOSCALING DURING TROUGH CONDITIONS

Figure 3

of autoscaling. For 2226 ionograms the parameters foF2, M(3000), MUF(3000), foF1, h'F, h'F2, fminF, fmin, foE, foEs, h'E and h'Es were investigated for their accuracy. The BISA program separates the E-region parameters into day and night groups to independently assess the accuracy of night E scaling. Ionograms with technical errors were removed from the data base.

5.1.1 foF2

The critical frequency of the F2 layer is perhaps the most important ionospheric parameter. The minimum accuracy requirement for a high latitude station like Goose Bay was set to ±1 MHz for 80% of all ionograms. Figures 4 to 7 show the error distributions for the selected four months. It can be seen that the minimum requirement is by far exceeded. The 1 MHz error limit test is passed by 92% of the ionograms in January, 96% in April, 97% in July and in September. Indeed, 90% of all ionograms satisfy the 0.5 MHz error limit. The curves on the left side of the figures show the symmetry of the error distribution which is more or less Gaussian in shape. The error statistics for the ionograms without spread F, e.e., daytime ionograms, were established separately. It is satisfying to see that the error curves for all ionograms (dashed curves) are only about 10% lower than those for non-spread ionograms (solid curves).

5.1.2 MUF(3000)

Figures 8 to 11 display the error distribution function of MUF(3000) where the error is defined as the percentage difference between the manual and autoscaled value based on the manual reading. In July and September, over 90% of all ionograms have less than 10% errors, in April 88% and in January 80%. Averaged over the four months, 88% of all ionograms are scaled with a MUF(3000) value of less than 10%. If only non-spread ionograms are considered, the statistics of all months improve to 96%.

A clarification about our definition of MUF(3000) is in place here. In the BISA program the F region h'(f) curve is

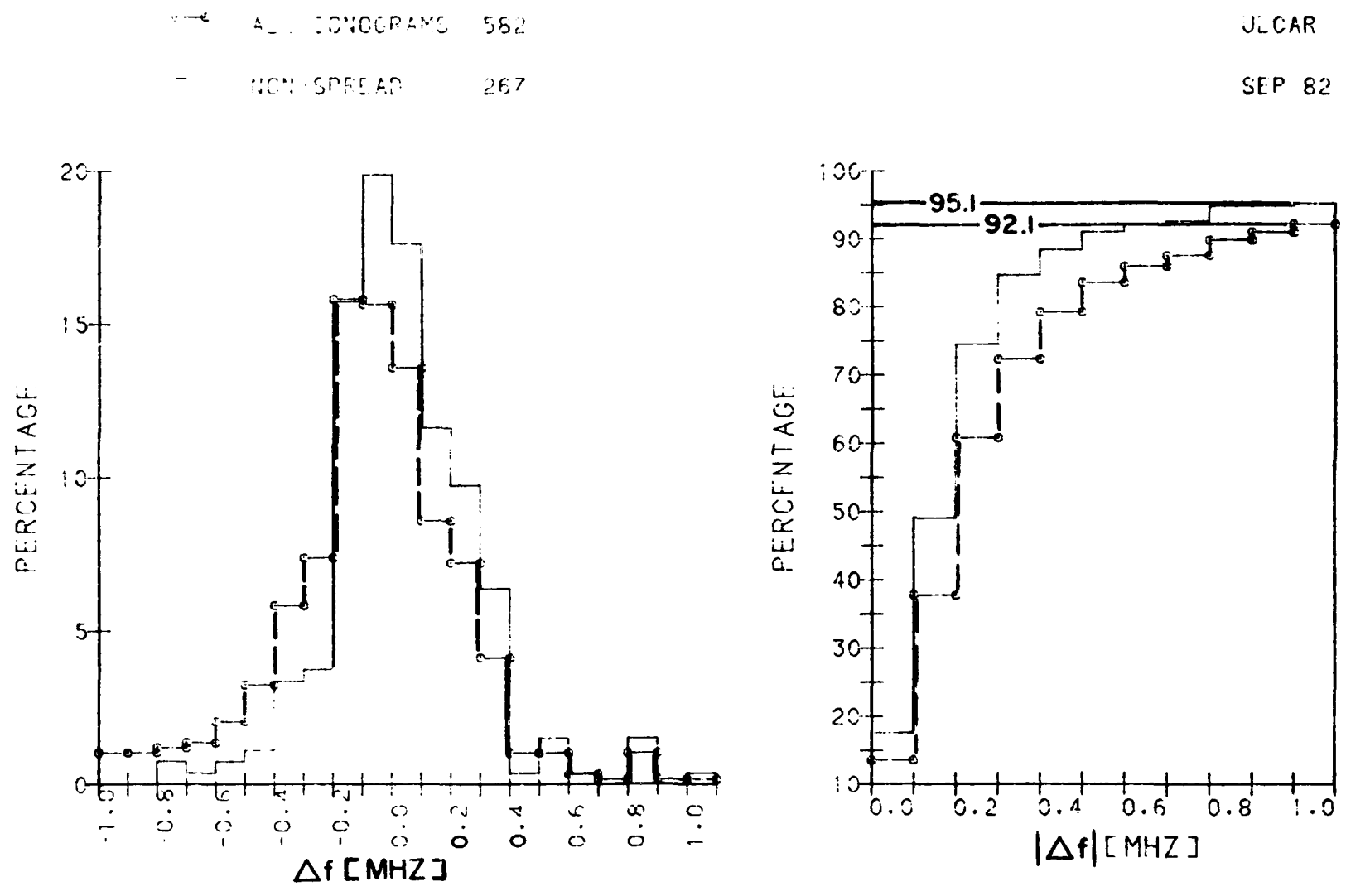

Figure 4

ERROR DISTRIBUTION OF FOF2 (MANUAL - AUTO FOF2)
JANUARY 1980 GOOSE BAY, LABRADOR

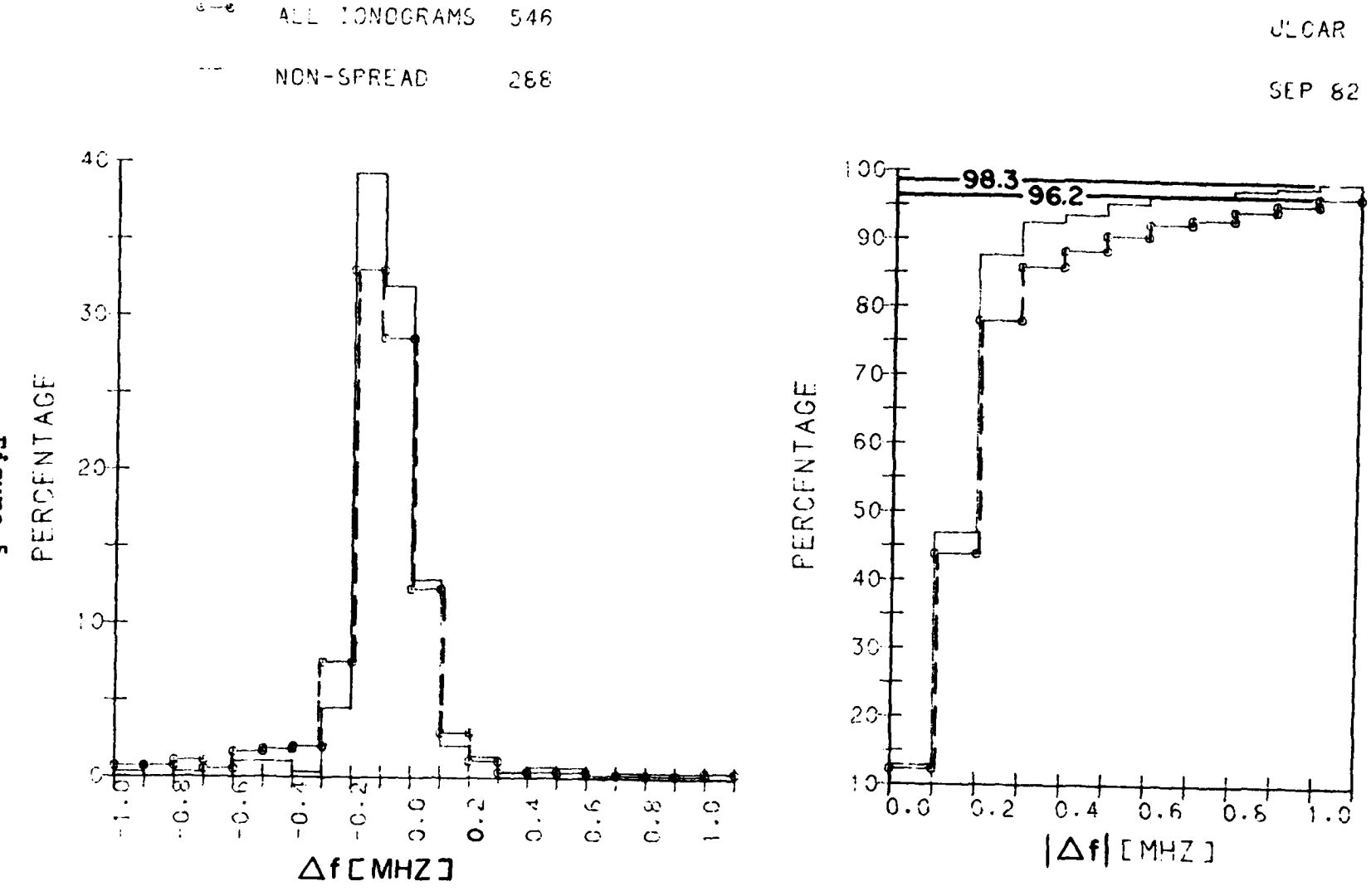

Figure 5

ERROR DISTRIBUTION OF FOF2 (MANUAL - AUTO FOF2)
APRIL 1980 GOOSE BAY, LABRADOR

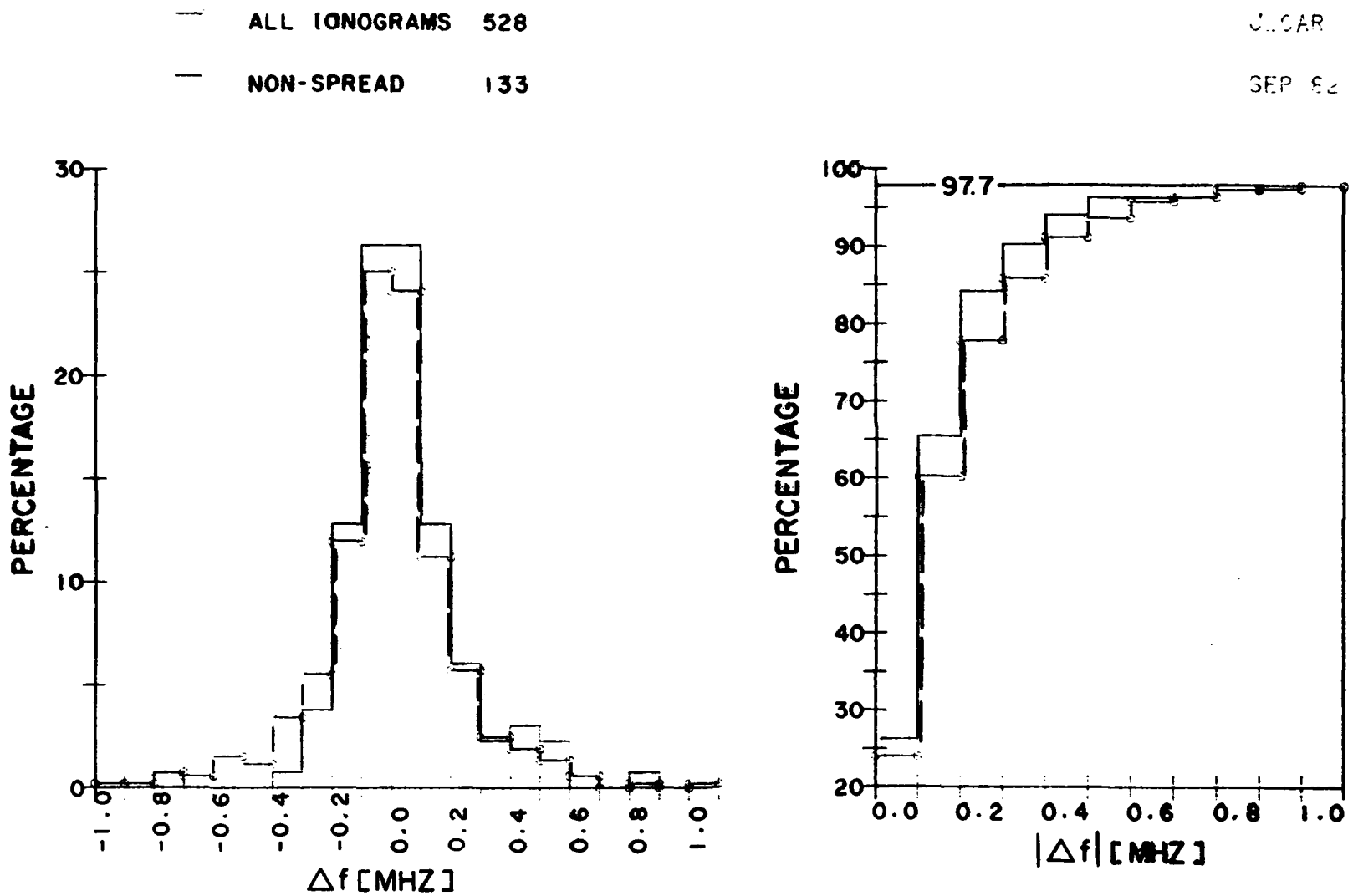

Figure 6

ERROR DISTRIBUTION OF FOF2 (MANUAL - AUTO FOF2)
JULY 1980 GOOSE BAY, LABRADOR

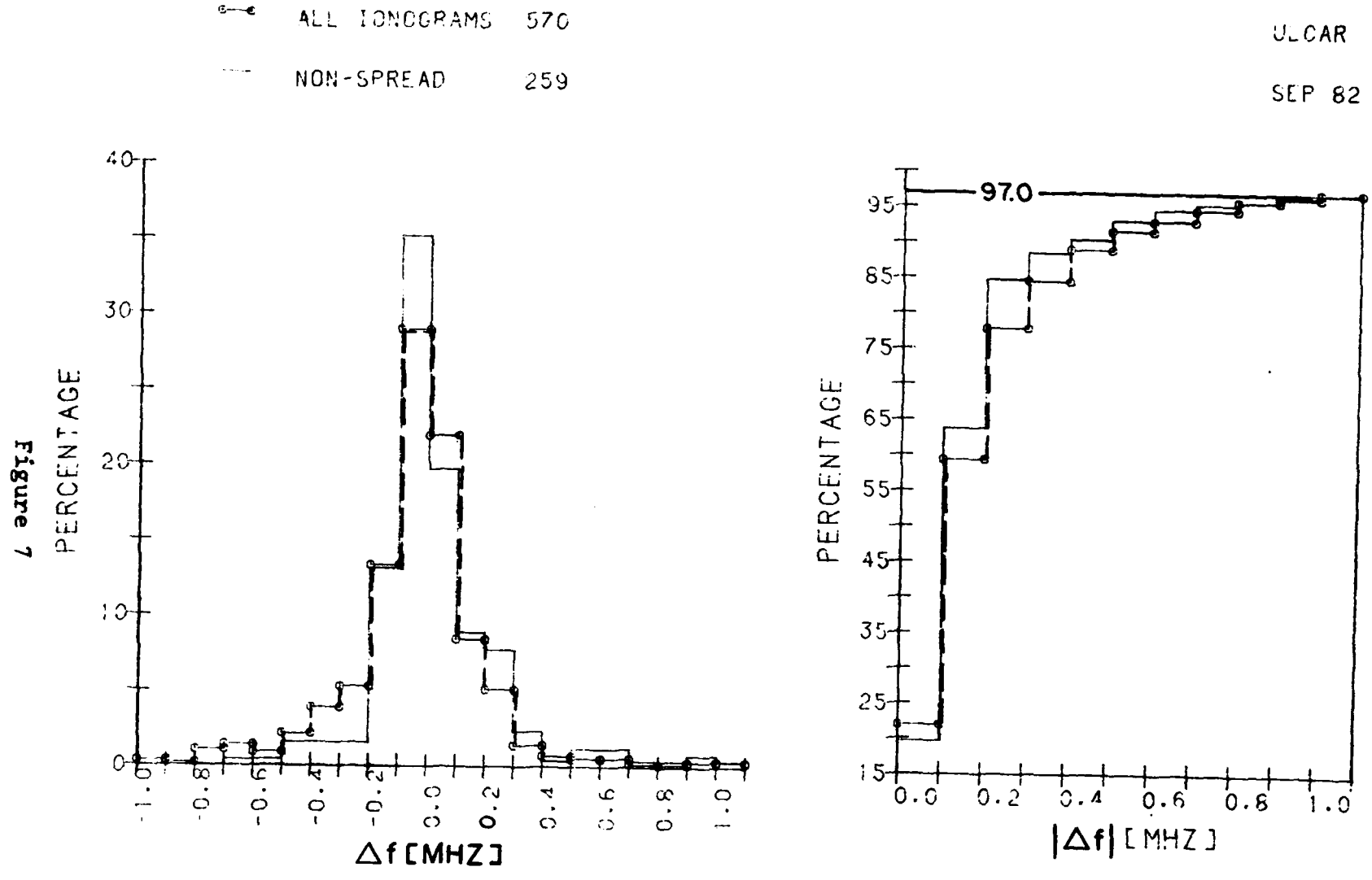

Figure 7

ERROR DISTRIBUTION OF FOF2 (MANUAL - AUTO FOF2)
SEPTEMBER 1980 GOOSE BAY, LABRADOR

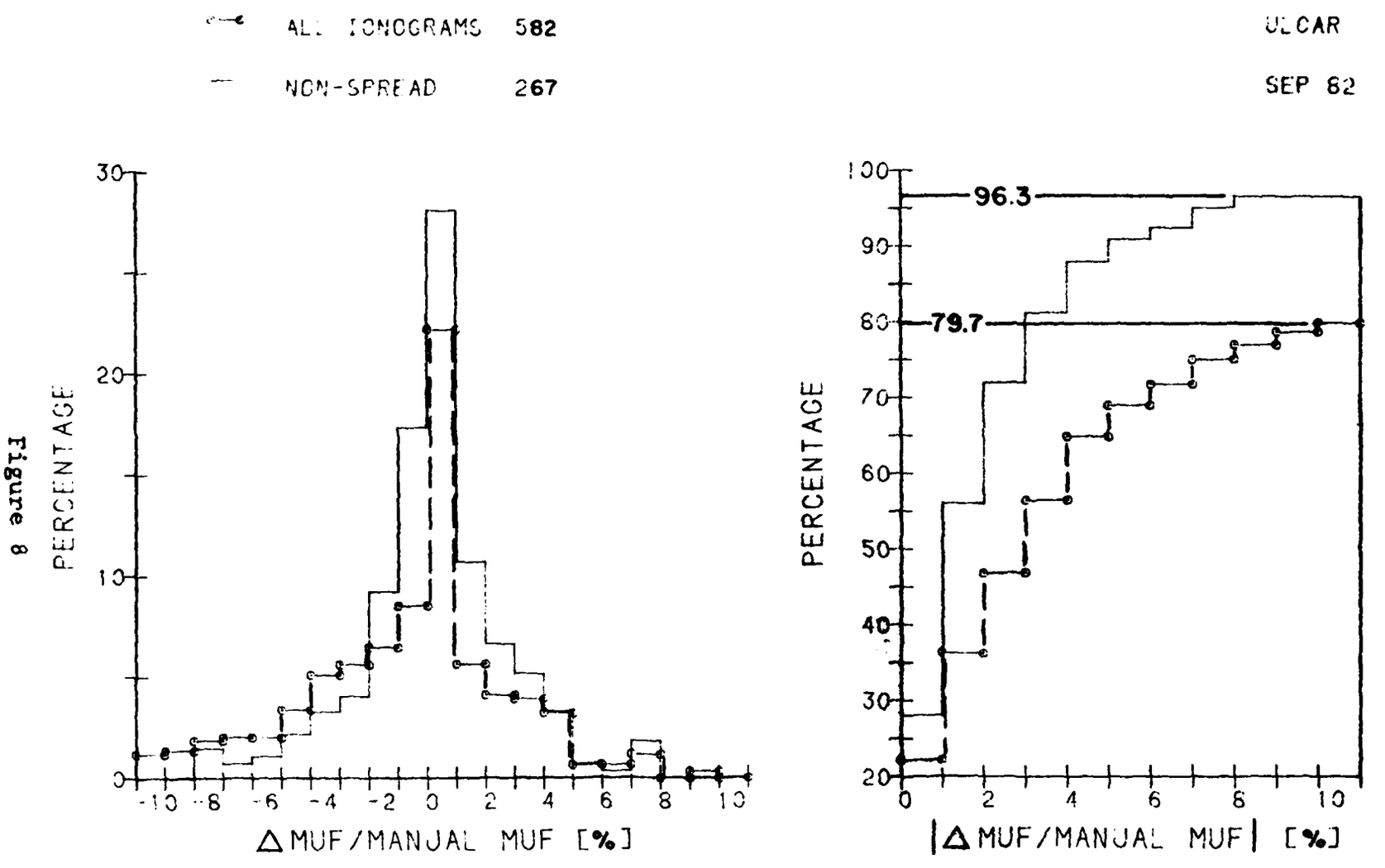

Figure 8

ERROR DISTRIBUTION OF MUF(3000) [(MANUAL MUF - AUTO MUF)/MANUAL MUF]
JANUARY 1980 GOOSE BAY, LABRADOR

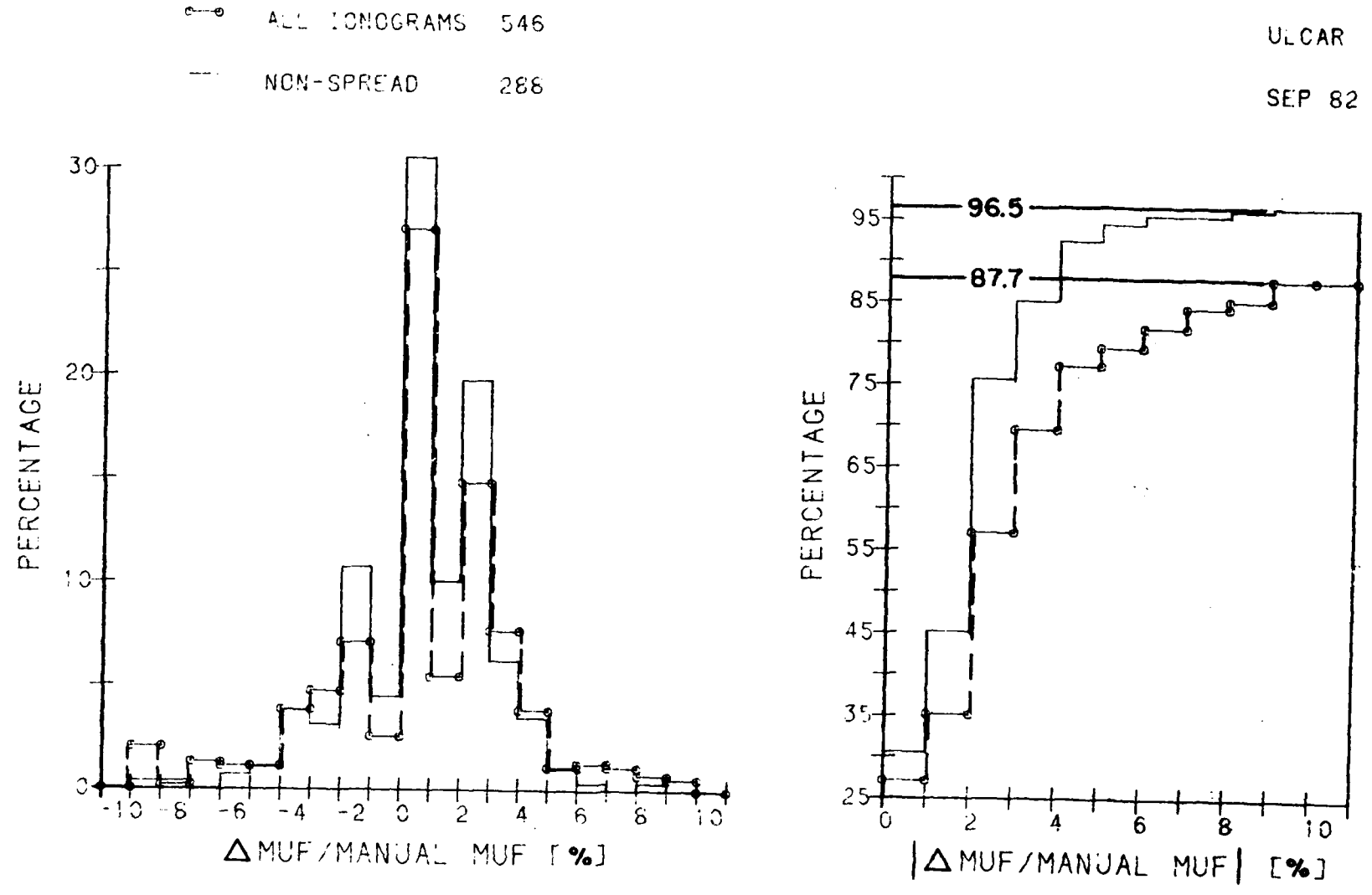

Figure 9

ERROR DISTRIBUTION OF MUF(3000) [(MANUAL MUF - AUTO MUF)/MANUAL MUF]
APRIL 1980 GOOSE BAY, LABRADOR

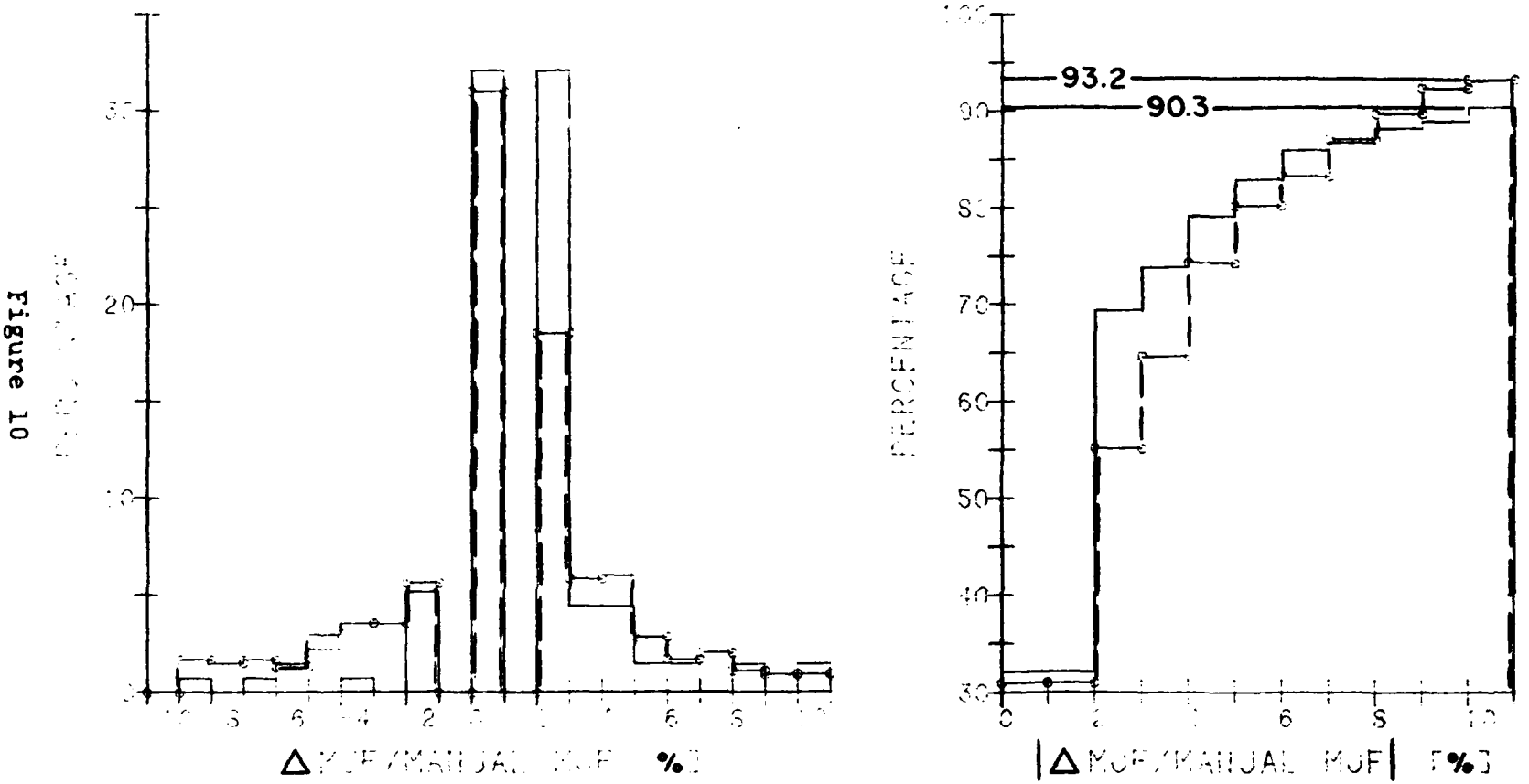

Figure 10

ERROR DISTRIBUTION OF MUF(3000) [(MANUAL MUF - AUTO MUF)/MANUAL MUF]
JULY 1980 GOOSE BAY, LABRADOR

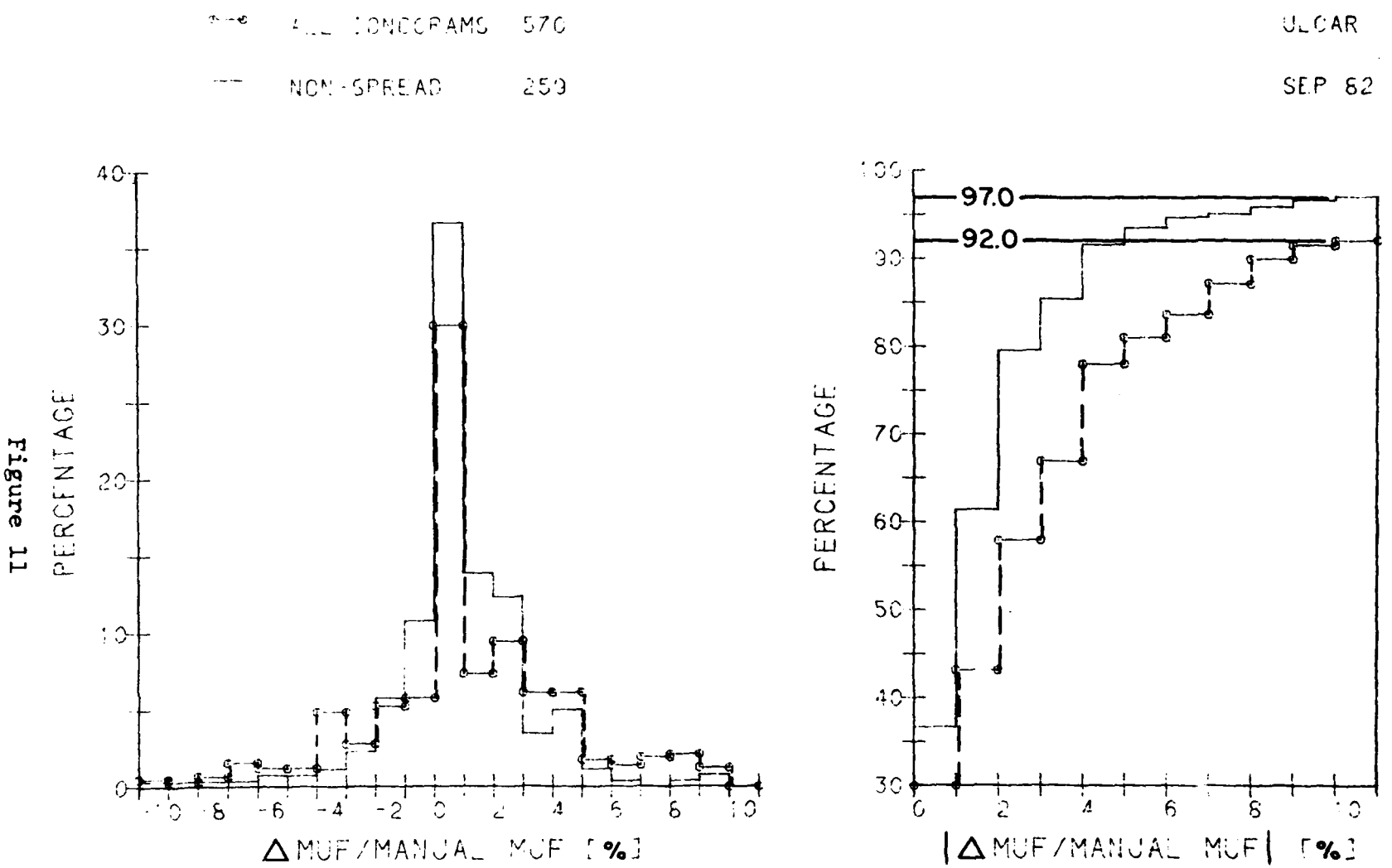

Figure 11

ERROR DISTRIBUTION OF MUF(3000) [(MANUAL MUF - AUTO MUF)/MANUAL MUF]
SEPTEMBER 1980 GOOSE BAY, LABRADOR

transformed into an oblique ionogram by multiplying each frequency with the transmission factor M(h')

$$f_{ob} = M(h')f_{vert}.$$

The transmission function M(h') is calculated for a distance of 3000 km by fitting a polynomial to the URSI specified data set [URSI Handbook of Ionogram Interpretation and Deduction, Second Edition, Nov. 1972, p. 21; World Data Center A Report UAG-23]. The maximum f_{ob} thus obtained is defined as MUF(3000) in the present BISA program. This may be either the MUF F1 or the MUF F2 whichever is larger. For the error statistics the comparison was therefore made with the larger of the MUF F1/MUF F2 values. It might be advisable in the future to autoscale always MUF F2, which could easily be done. The significantly higher percentage rates for the non-spread ionograms indicates the uncertainty in the MUF definition for spread ionograms.

5.1.3 M(3000)

The M(3000) propagation factor is derived from the MUF(3000), as defined in 5.1.2, by dividing it by foF2. The error distribution functions are shown in Figures 12 to 15. The minimum accuracy requirement of $\Delta M = \pm 0.2$ is fulfilled for 82% of all ionograms. In January, which had the highest magnetic activity, only 78% of all ionograms pass the 0.2 error test. For the other three months the percentages are above 81%.

5.1.4 Average Diurnal Variation of the Scaling Accuracy

The percentage of ionograms that were scaled with an foF2 error of less than 1 MHz is plotted as function of local time in Figures 16 to 19. Not surprisingly, the best results are obtained for the daytime ionograms which in the average are less disturbed. January shows a marked difference at night between the percentage curves for all and the non-spread ionograms. The same behavior is

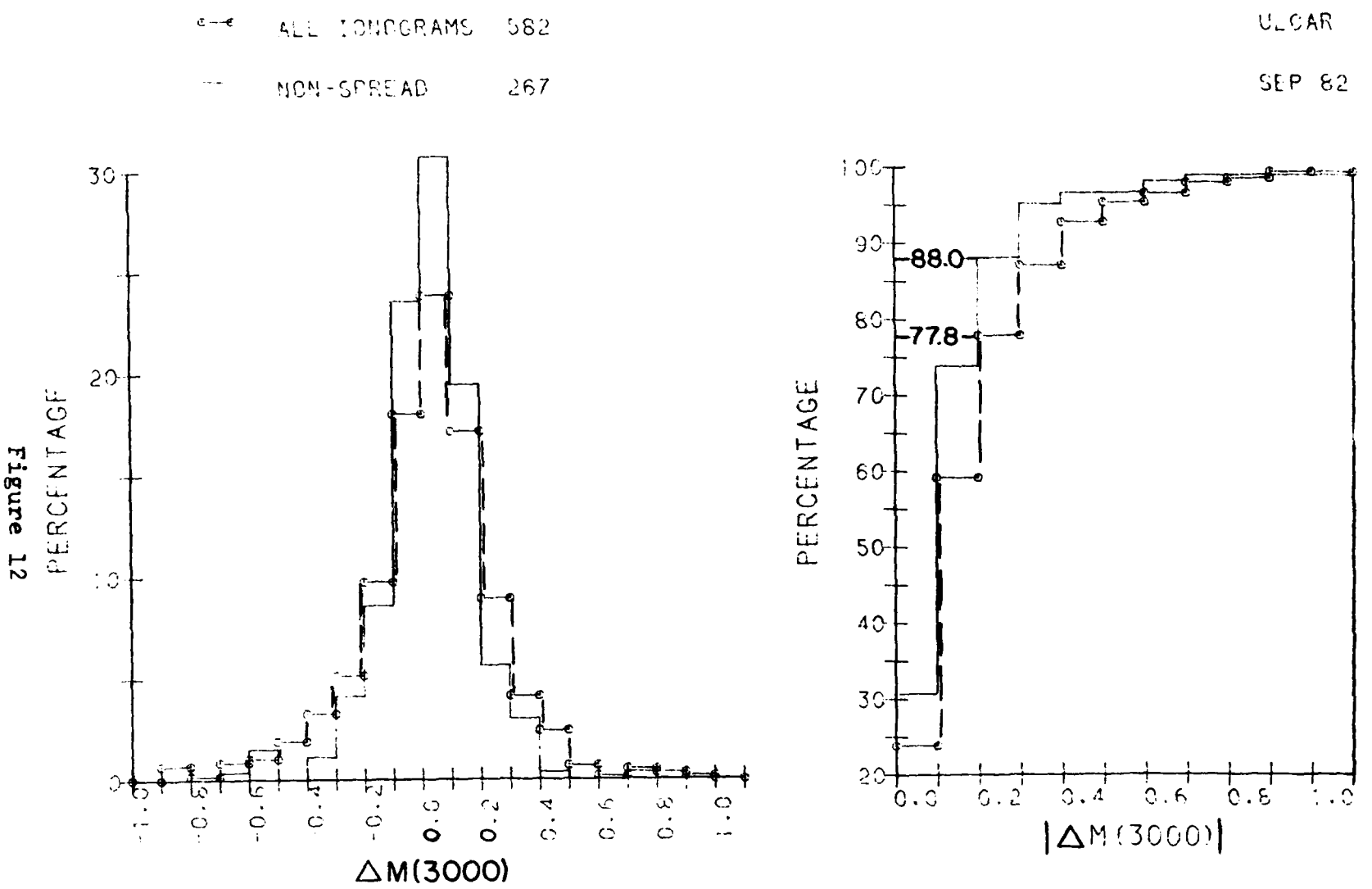

Figure 12

ERROR DISTRIBUTION OF M(3000) [MANUAL M(3000) - AUTO M(3000)]
JANUARY 1980 GOOSE BAY, LABRADOR

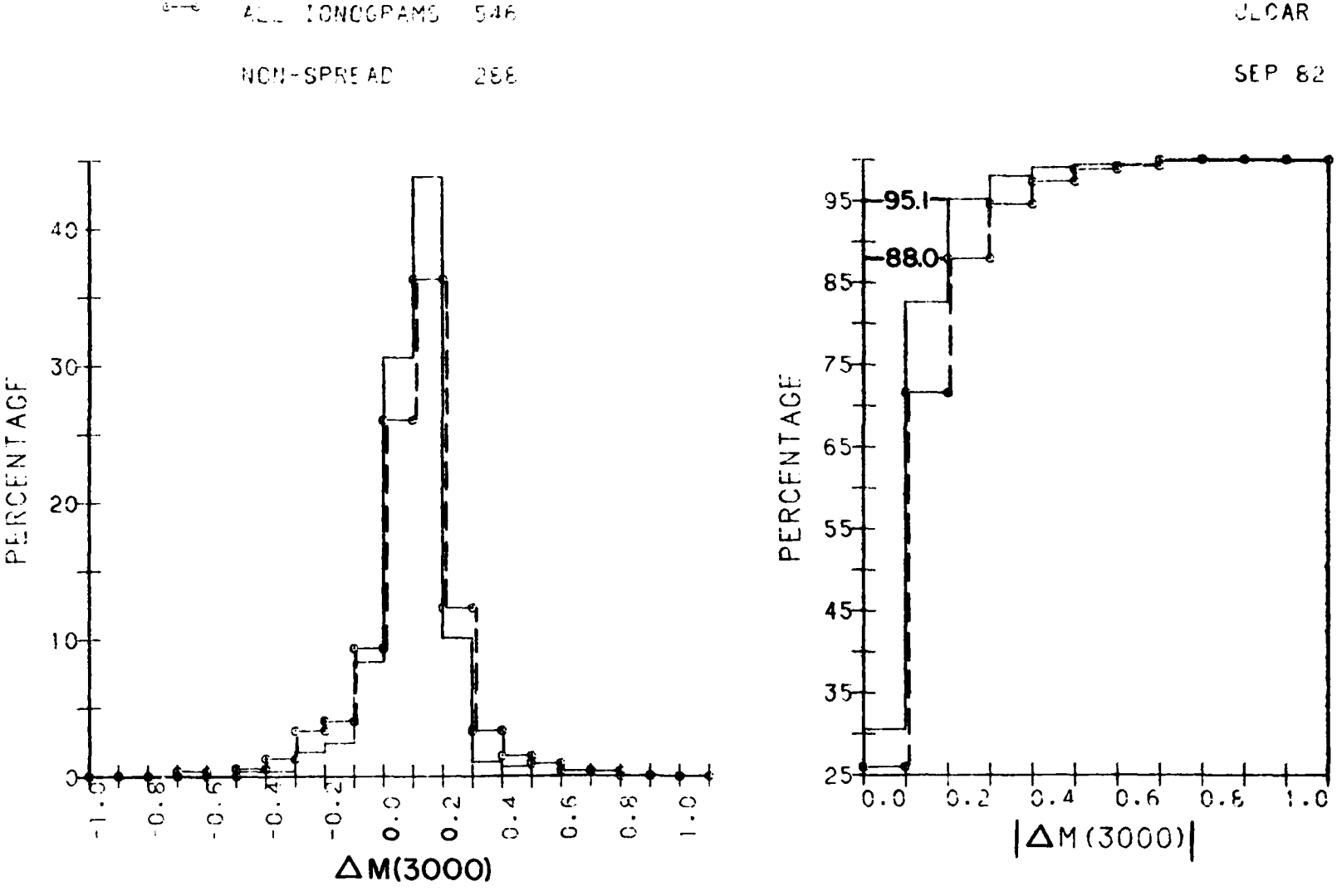

Figure 13

ERROR DISTRIBUTION OF M(3000) [MANUAL M(3000) - AUTO M(3000)]
APRIL 1980 GOOSE BAY, LABRADOR

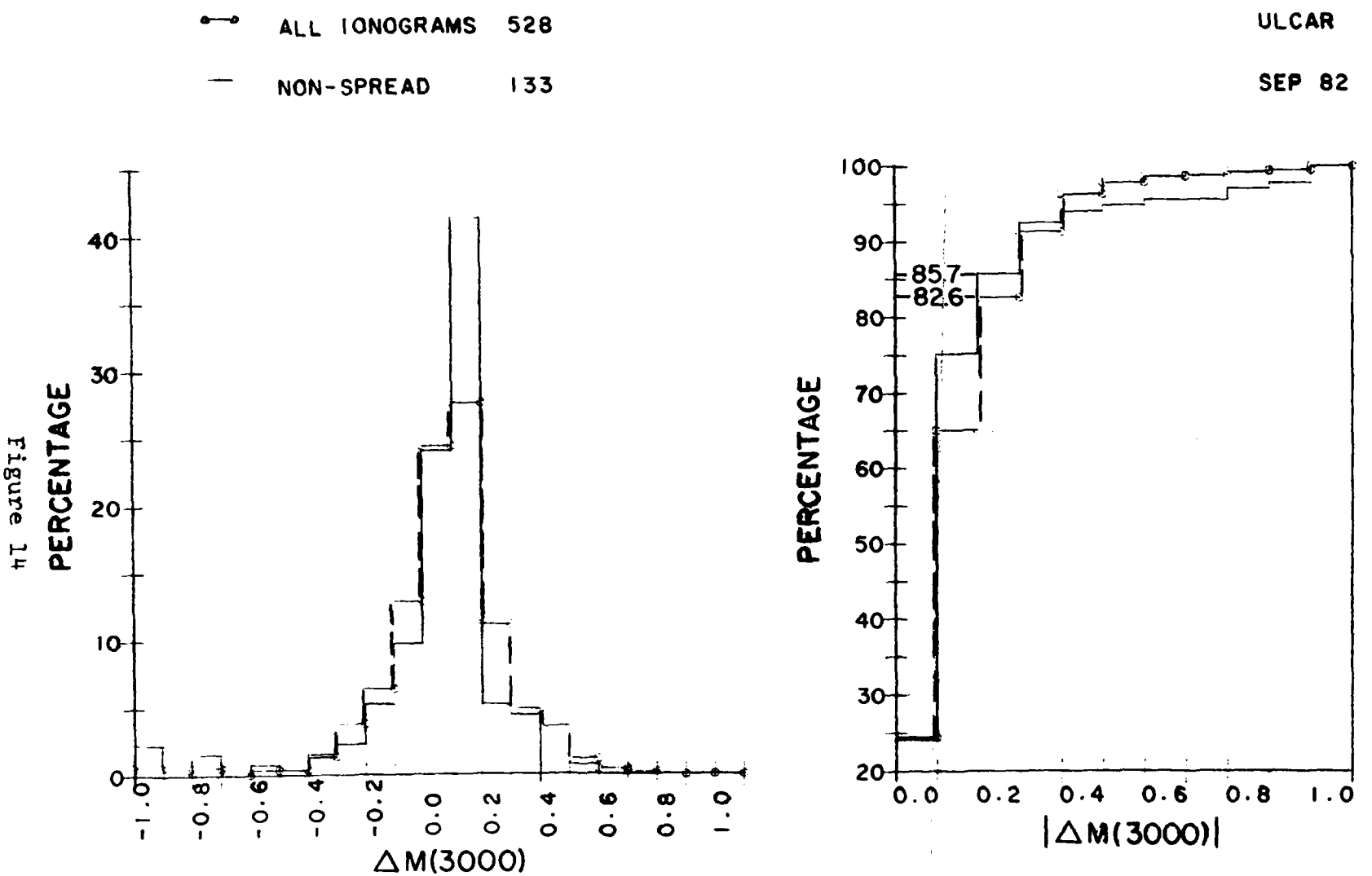

Figure 14

ERROR DISTRIBUTION OF M(3000) [MANUAL M(3000) - AUTO M(3000)]
JULY 1980 GOOSE BAY, LABRADOR

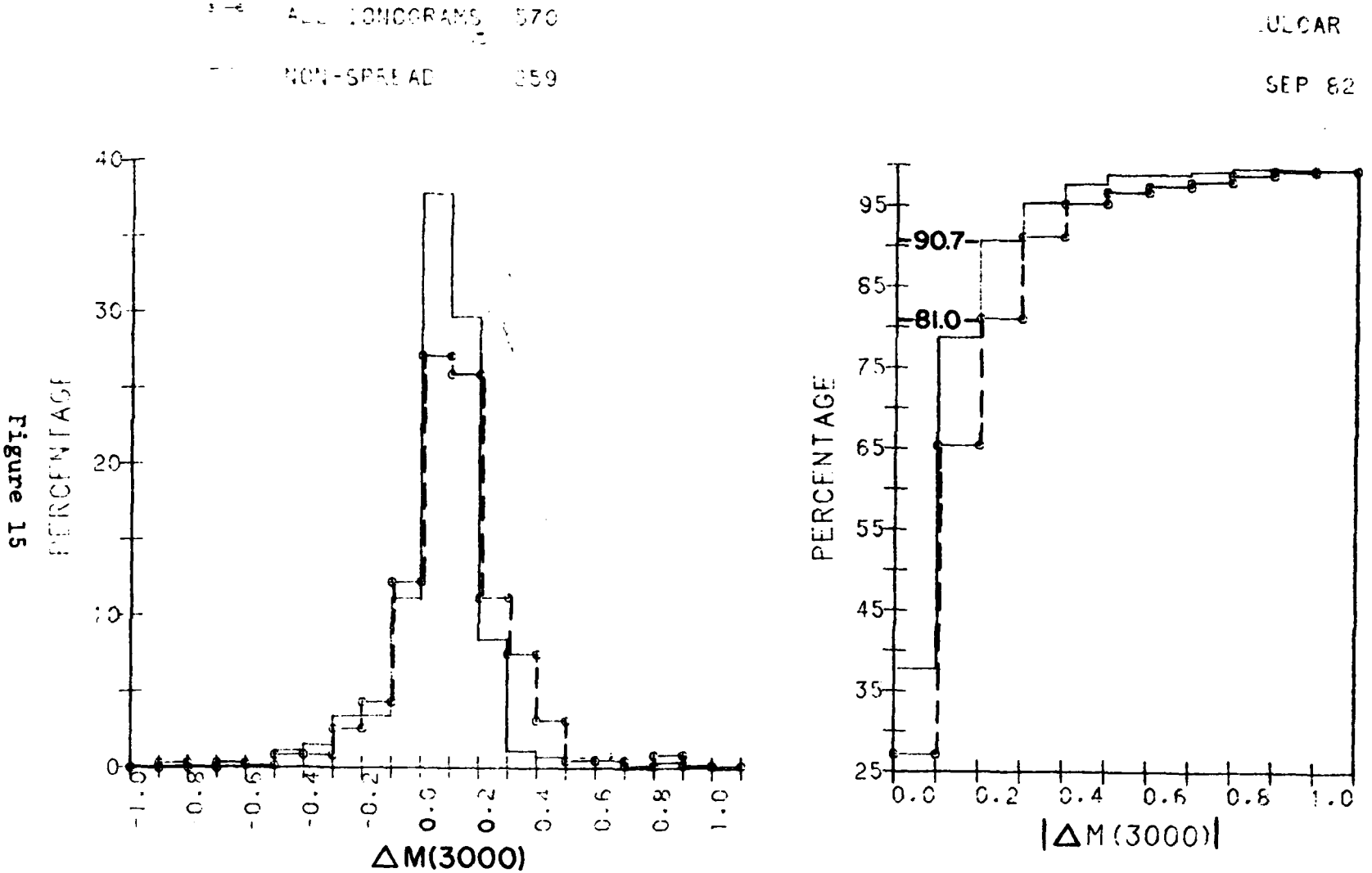

Figure 15

ERROR DISTRIBUTION OF M(3000) [MANUAL M(3000) - AUTO M(3000)]
SEPTEMBER 1980 GOOSE BAY, LABRADOR

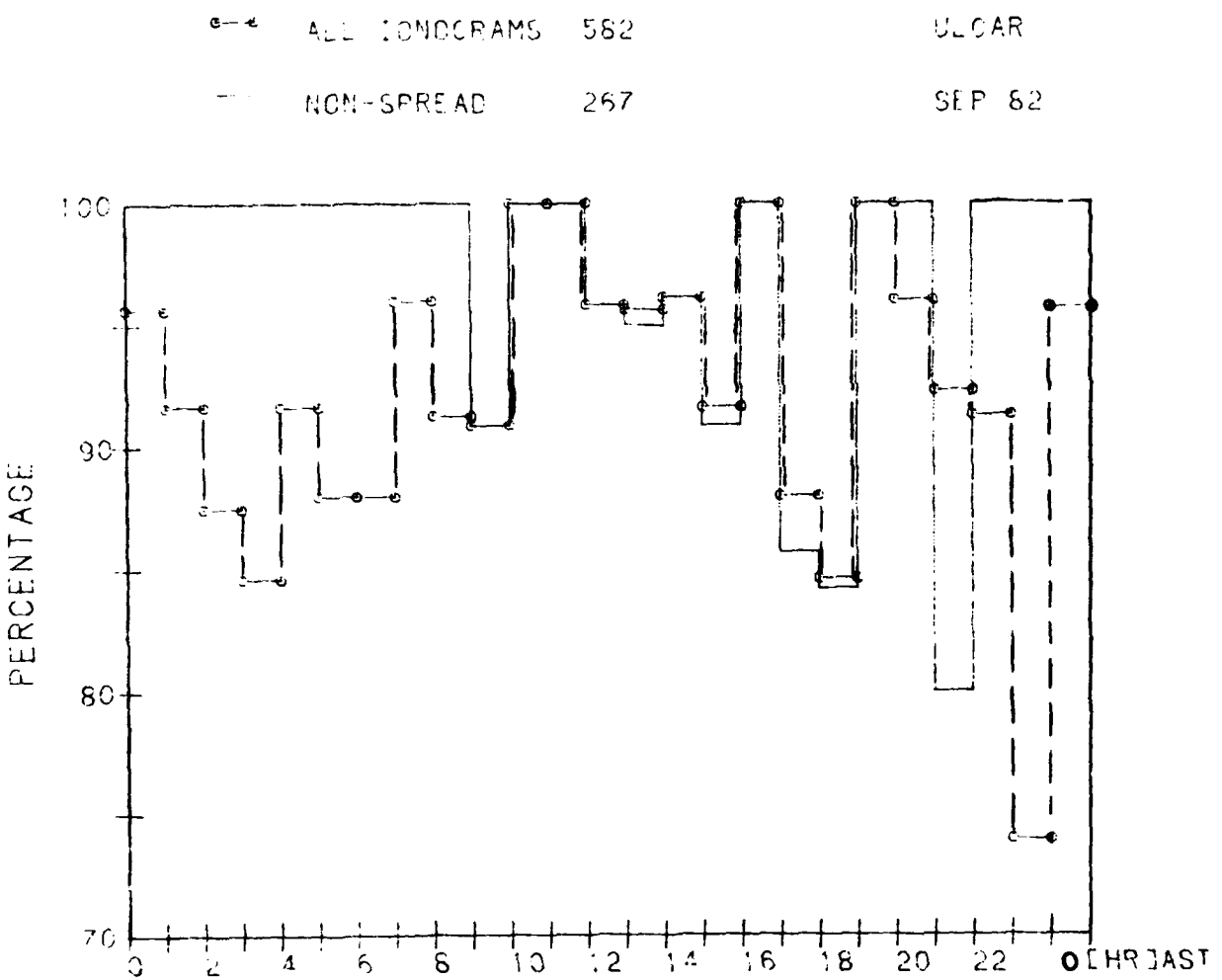

DIURNAL VARIATION OF 1 MHZ ERROR LIMIT FOR foF2

|MANUAL FOF2 - AUTO FOF2|
JANUARY 1980 GOOSE BAY, LABRADOR

Figure 16

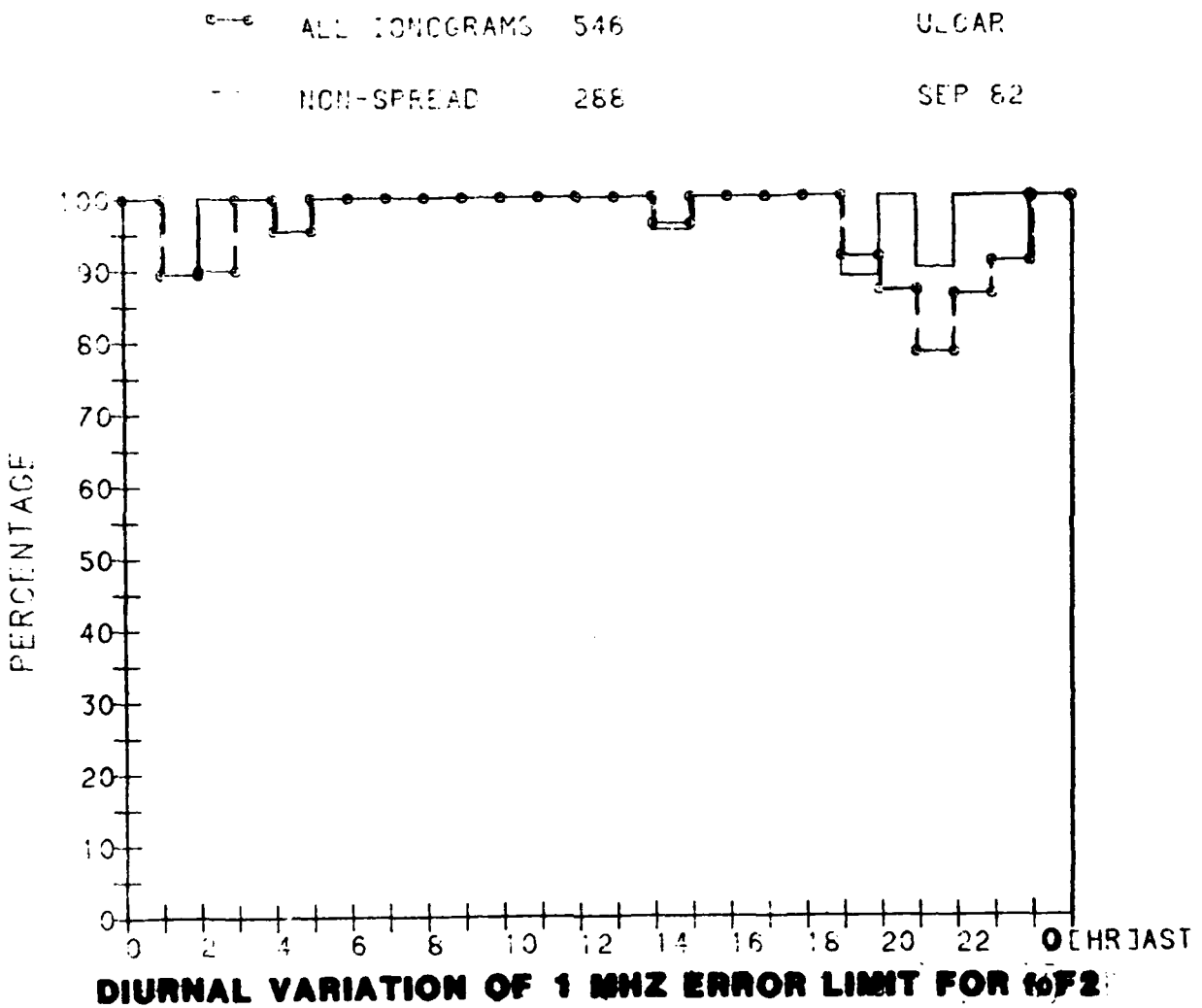
ALL IONOGRAMS 546
NON-SPREAD 288
ULCAR
SEP 82
PERCENTAGE
100
90
80
70
60
50
40
30
20
10
0
0 2 4 6 8 10 12 14 16 18 20 22
0 CHR JAST
DIURNAL VARIATION OF 1 MHZ ERROR LIMIT FOR foF2
|MANUAL FOF2 - AUTO FOF2|
APRIL 1980 GOOSE BAY, LABRADOR

Figure 17

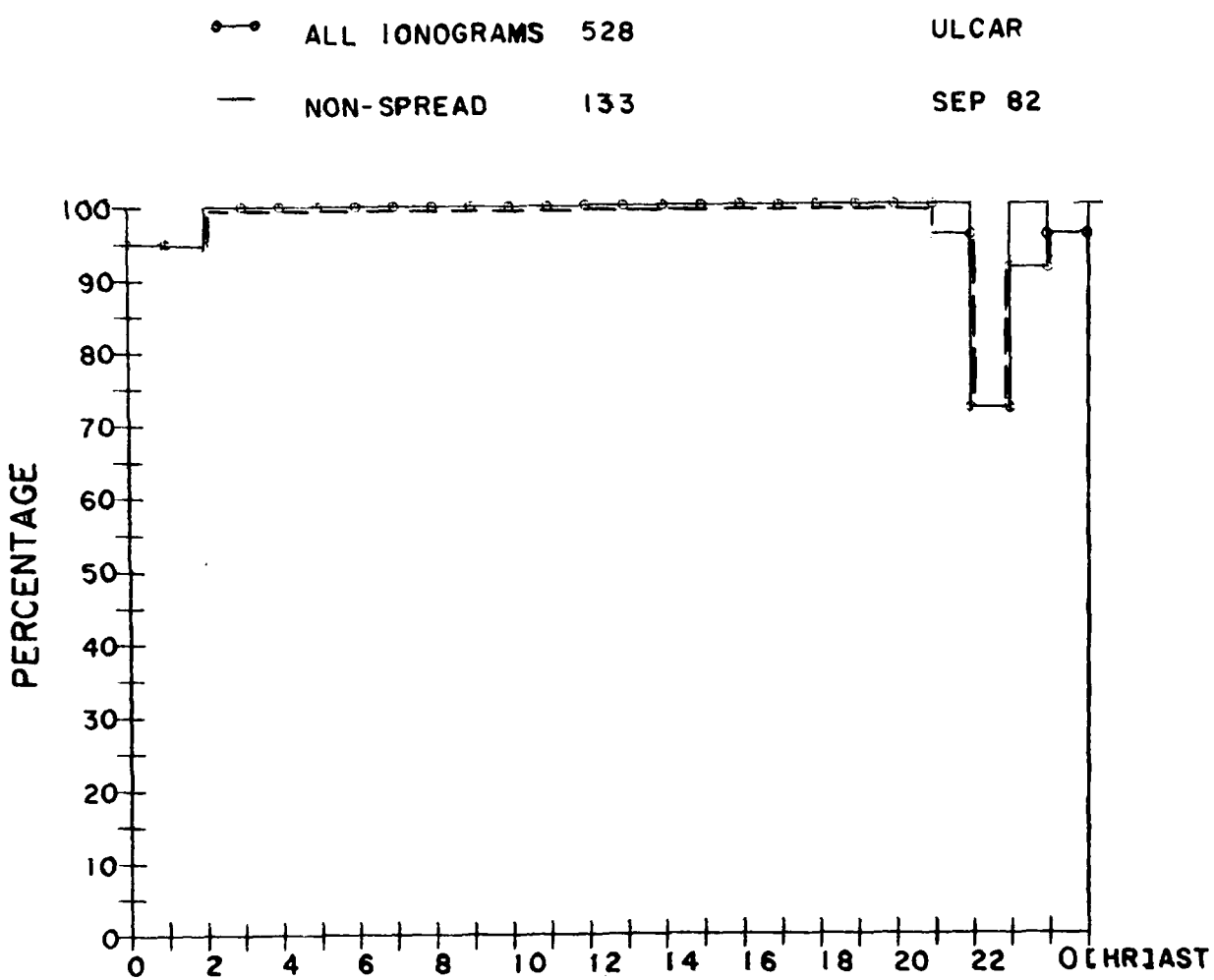

|MANUAL FOF2 - AUTO FOF2|
JULY 1980 GOOSE BAY, LABRADOR

Figure 18

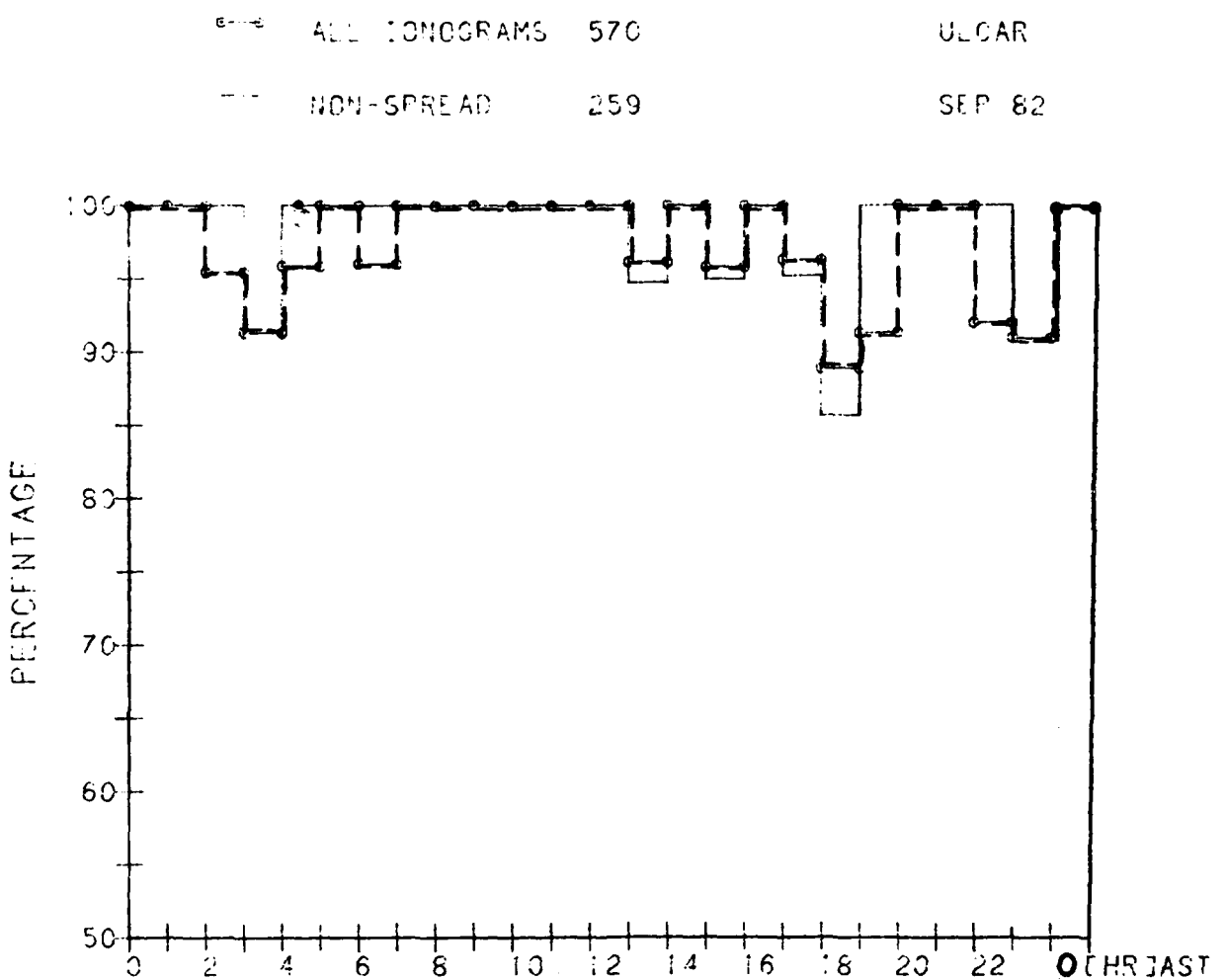

Figure 19

|MANUAL FOF2 - AUTO FOF2|
SEPTEMBER 1980 GOOSE BAY, LABRADOR

displayed by the MUF error curves (Figures 20 to 23) and the M-factor error curves (Figures 24 to 27).

5.2 Other Parameters and Statistical Summary

Table 1 summarizes the results for the parameters foF1, fminF, fmin, h'F and h'F2. No F1 layer was observed in January. One can see that only 69% of all ionograms are scaled within an h'F2 error of 10 km. This is caused by the fact that BISA simply lets the trace point $h'(f_m)$ with the lowest height for f_m > foF1 determine h'F2. The accuracy of this parameter can be improved by precisely determining the leading edge of the echo trace at $f \approx f_m$ in the raw ionogram. This method will also be applied to the h'F height. Table 2 lists the results for the E region parameters. The data are separated into day and night ionogram to better see the effect of the occurrence of night E [King, 1962] which is contained in the foE column. Since night E occasionally occurs already in the late afternoon the day/night transition was made when the predicted foE goes below 2.5 MHz. For more than 92% of the day ionograms the foE value is scaled within 0.2 MHz; the corresponding value is 71% for night E. For an error limit of 0.5 MHz, 88% of the night ionograms are successfully scaled. The autoscaled h'E values suffer somewhat because the E trace algorithm finds foE and h'E simultaneously, optimizing foE at the account of h'E. This parameter will be improved by the same method discussed above for h'F2. The critical frequency of the sporadic E layer is autoscaled within 0.5 MHz of the manual value for 84% of the day and 69% of the night ionogram. The auto values for foEs are consistently lower than the manual readings. The reason is that BISA searches for a continuous trace of vertical O-echoes and terminates the trace when there are no O-echoes within 300 kHz. The manual scaler often extends the trace if the O-gaps are filled with oblique and X-echoes.

Finally, Table 3 is a summary of the results discussed earlier for foF2, MUF(3000) and M(3000).

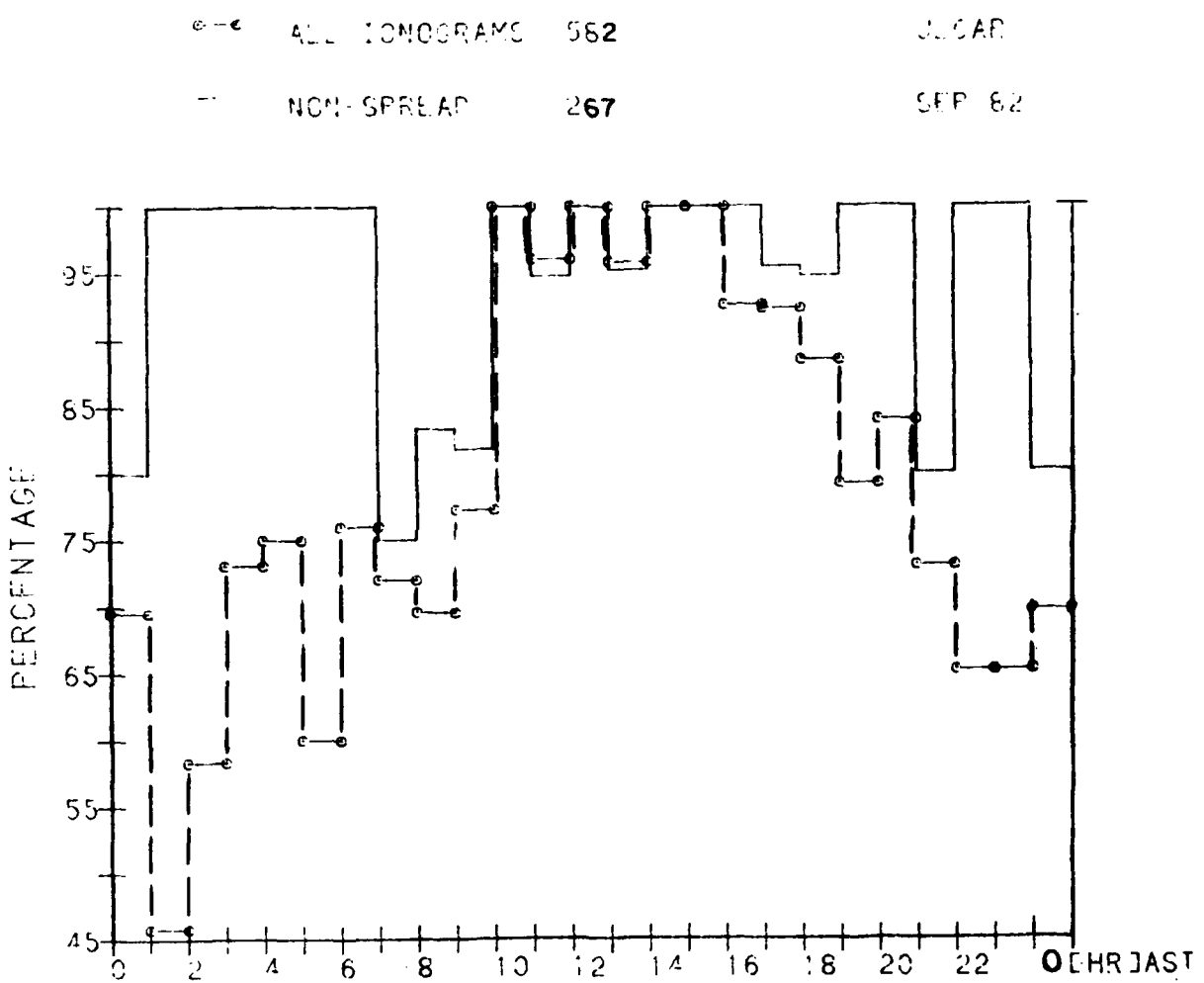

Figure 20

| MANUAL MUF - AUTO MUF | /MANUAL MUF
JANUARY 1980 GOOSE BAY, LABRADOR

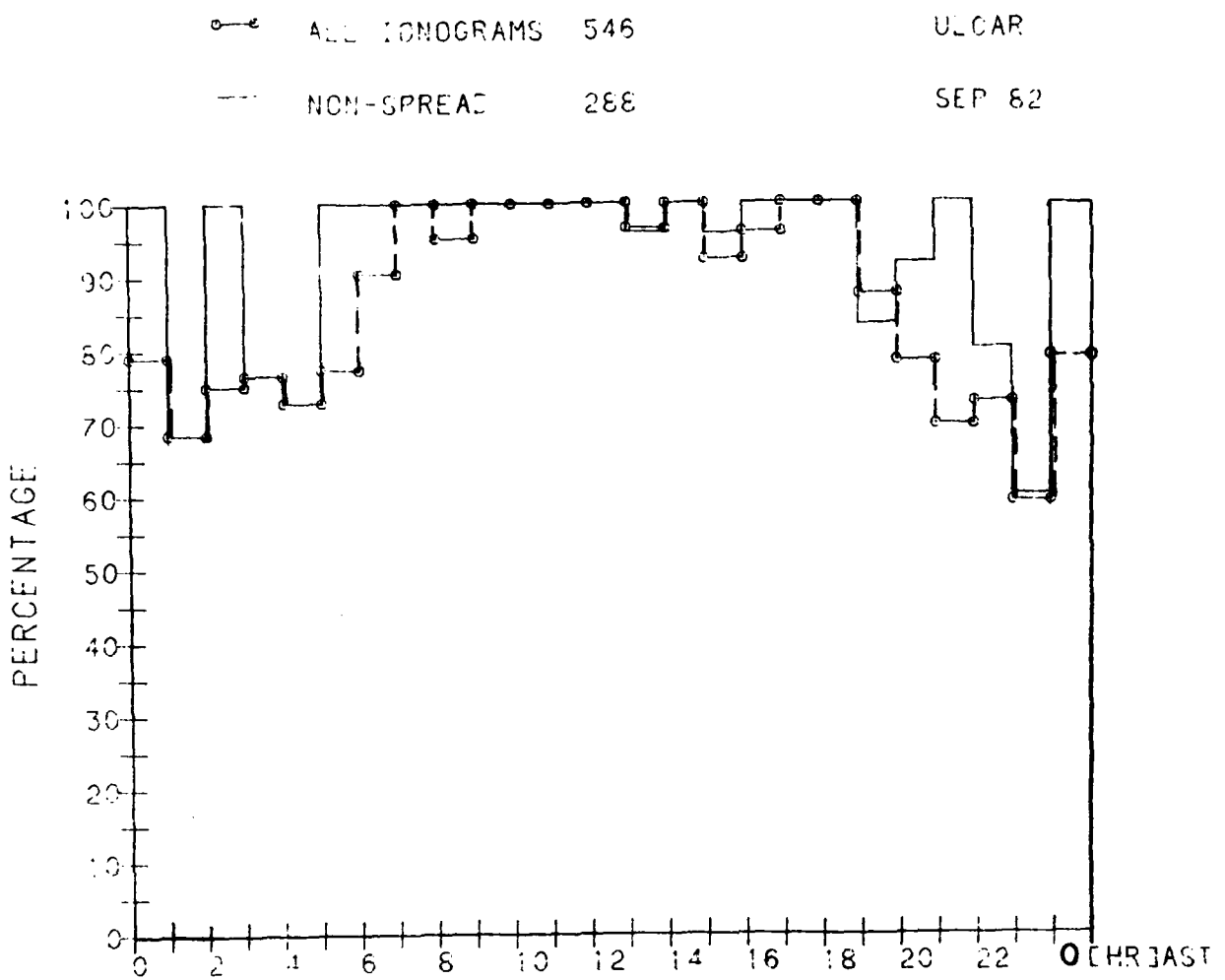

| MANUAL MUF - AUTO MUF | /MANUAL MUF
APRIL 1980 GOOSE BAY, LABRADOR

Figure 21

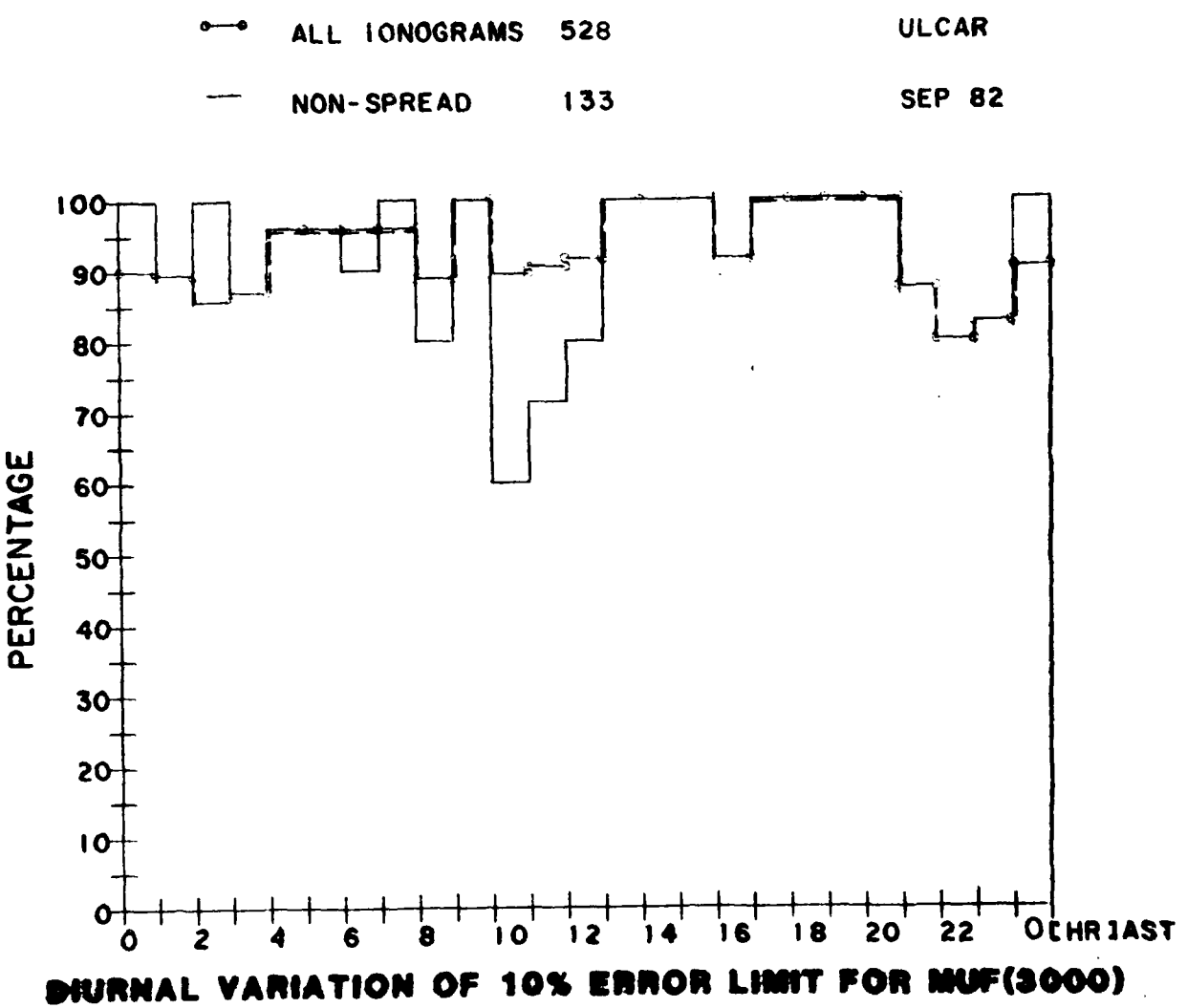

Figure 22

| MANUAL MUF - AUTO MUF | /MANUAL MUF
JULY 1980 GOOSE BAY, LABRADOR

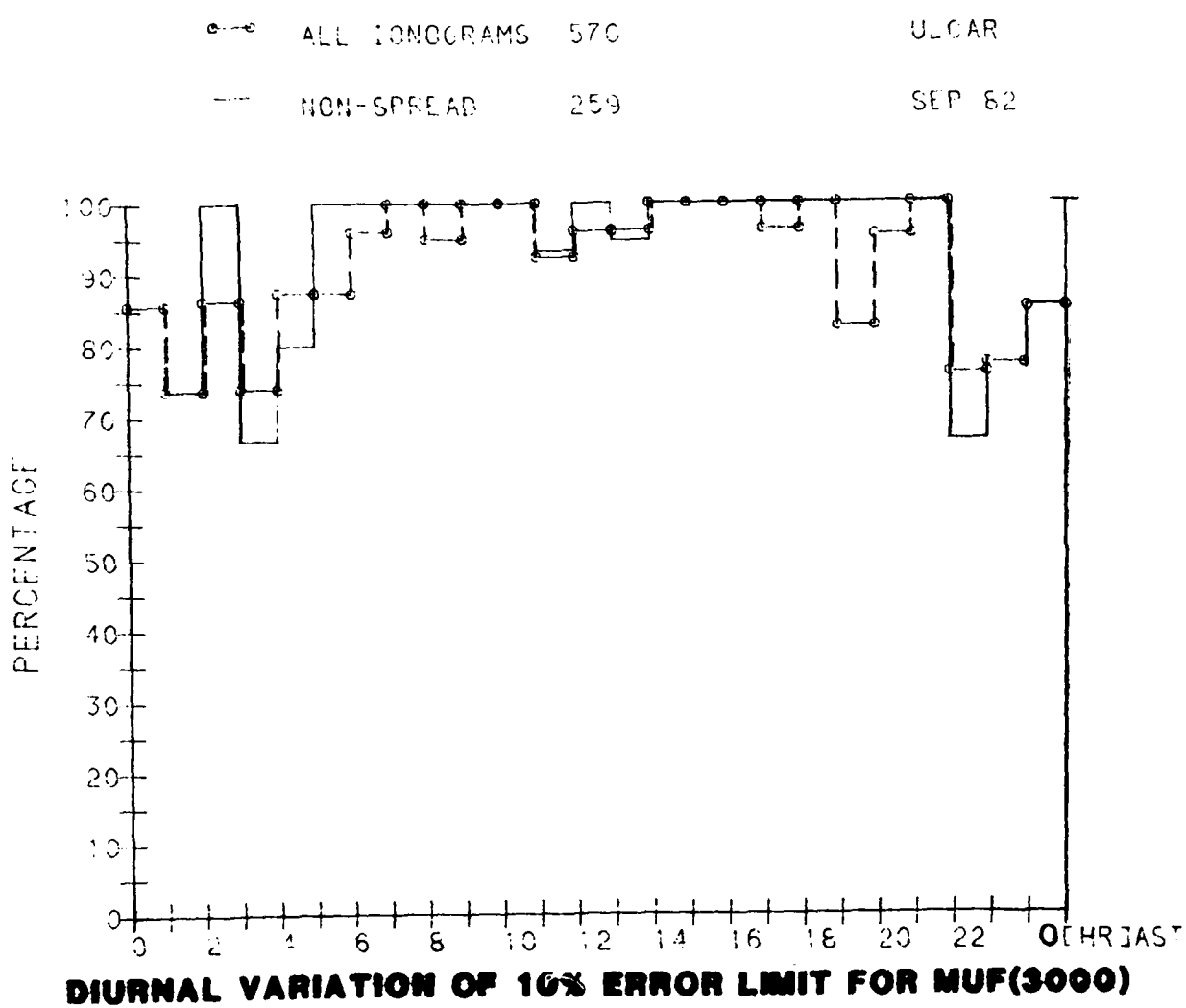

Figure 23

|MANUAL MUF - AUTO MUF| /MANUAL MUF
SEPTEMBER 1980 GOOSE BAY, LABRADOR

Figure 24

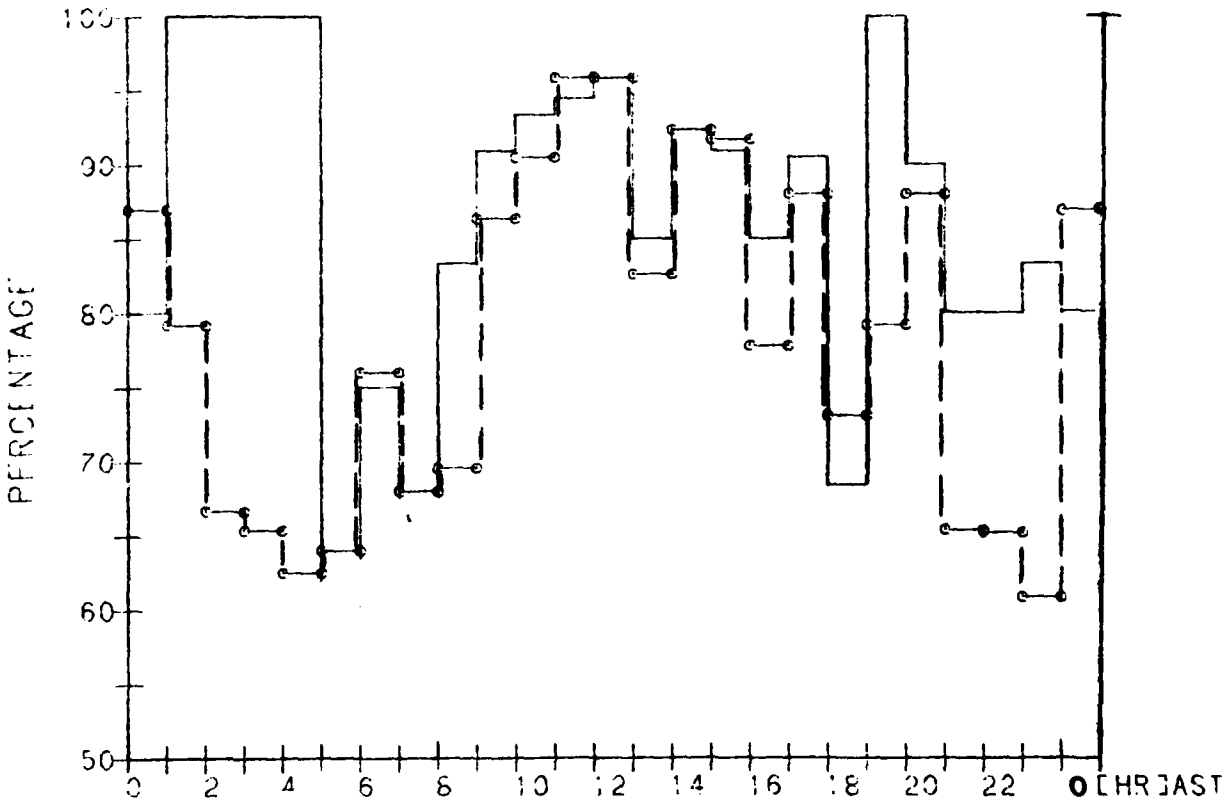

DIURNAL VARIATION OF .2 ERROR LIMIT FOR M(3000)

|MANUAL M(3000) - AUTO M(3000)|
JANUARY 1980 GOOSE BAY, LABRADOR

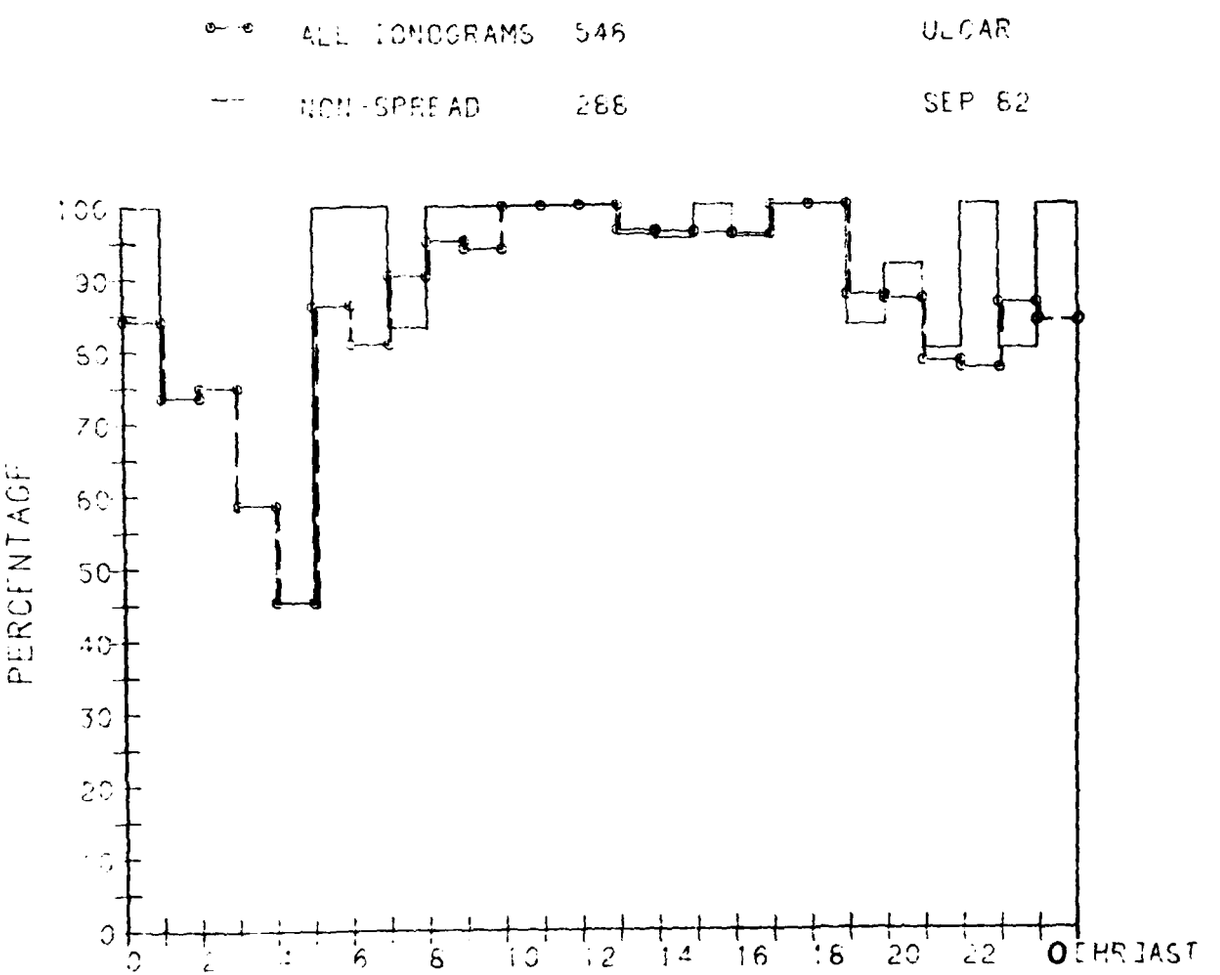

DIURNAL VARIATION OF .2 ERROR LIMIT FOR M(3000)

|MANUAL M(3000) - AUTO M(3000)|
APRIL 1980 GOOSE BAY, LABRADOR

Figure 25

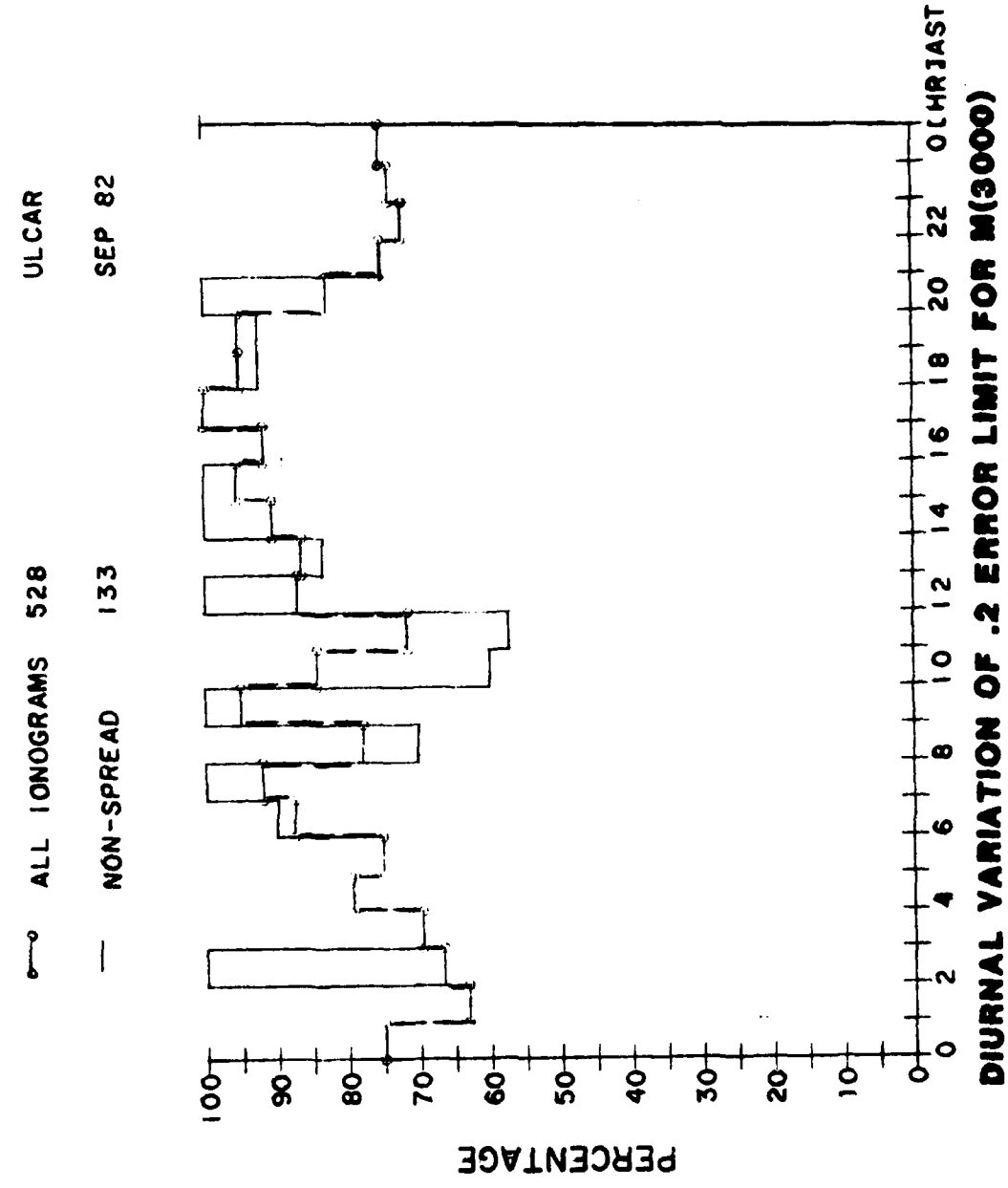
ULCAR
SEP 82
ALL IONOGRAMS 528
NON-SPREAD 133
DIURNAL VARIATION OF .2 ERROR LIMIT FOR M(3000)
O(HR)AST
0 2 4 6 8 10 12 14 16 18 20 22
PERCENTAGE
100 90 80 70 60 50 40 30 20 10
|MANUAL M(3000) - AUTO M(3000)|
JULY 1980 GOOSE BAY, LABRADOR

Figure 26

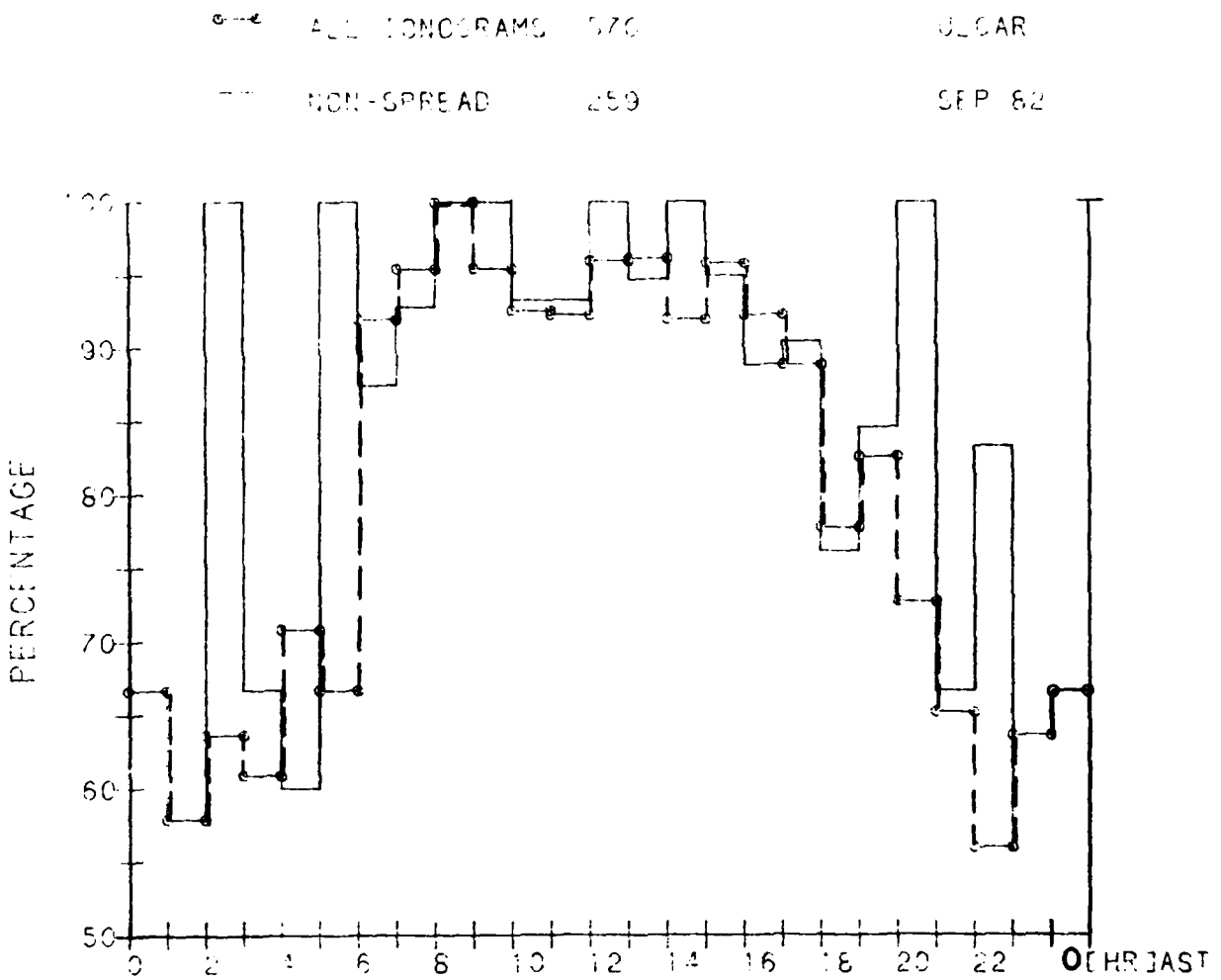

DIURNAL VARIATION OF .2 ERROR LIMIT FOR M(3000)

|MANUAL M(3000) - AUTO M(3000)|
SEPTEMBER 1980 GOOSE BAY, LABRADOR

Figure 27

F Region Statistics

Table 1

1980	No. of Ionograms	foF1(%) MHz ±0.2	foF1(%) MHz ±0.5	fminF(%) MHz ±0.2	fminF(%) MHz ±0.5	fmin(%) MHz ±0.5	fmin(%) MHz ±1.0	h'F(%) km ±10	h'F(%) km ±20	h'F2(%) km ±10	h'F2(%) km ±20
January	589	No F1 trace		80.8	95.3	71.7	96.2	88.1	93.9	----	----
April	556	68.8	93.5	74.3	93.6	79.4	94.3	88.1	94.6	72.7	84.4
July	525	85.0	97.9	67.7	89.7	50.0	93.0	75.2	86.1	62.7	73.9
September	570	84.8	97.0	84.1	95.8	77.9	95.1	86.1	94.6	81.8	87.9
Four Months	2240	80.0	96.4	76.9	93.7	69.9	94.7	84.6	92.4	68.8	79.6

F Region Statistics

Table 2

	1980	No. of Ionograms	FoE(%) MHz ±0.2	FoE(%) MHz ±0.5	h'E(%) km ±10	h'E(%) km ±15	foEs(%) MHz ±0.2	foEs(%) MHz ±0.5	h'Es(%) km ±10	h'Es(%) km ±15
Day Ionograms	January	589	97.3	100.0	65.8	80.2	74.1	88.4	75.0	86.6
	April	259	91.1	99.6	62.0	83.7	72.2	93.8	62.6	82.6
	July	303	90.3	98.3	64.0	88.7	47.2	71.0	64.7	81.9
	September	220	96.3	99.5	62.8	82.6	75.0	88.6	60.0	80.9
	Four Months	894	92.9	99.2	63.4	84.7	64.7	84.1	64.2	82.4
Night Ionograms	January	348	80.1	93.0	73.0	83.4	63.8	77.3	73.3	81.0
	April	278	70.4	87.3	68.9	80.2	54.3	73.0	63.7	71.4
	July	241	56.9	81.7	47.9	65.0	32.0	46.9	67.4	75.7
	September	334	72.4	90.8	63.6	79.2	56.9	74.0	69.1	79.6
	Four Months	1201	70.9	88.7	64.4	77.8	53.3	69.3	68.7	77.3

foF2 and MUF Statistics

Table 3

1980	No. of Ionograms	foF2(%) MHz ±0.5	foF2(%) MHz ±1.0	MUF(3000)(%) ±5%	MUF(3000)(%) ±10%	M(3000)(%) MHz ±0.1	M(3000)(%) MHz ±0.2	
January	582	83.5	92.1	69.0	79.7	59.1	77.8	All Ionograms
April	546	90.3	96.2	79.5	87.7	71.6	88.0	
July	528	93.6	97.7	80.2	93.2	65.0	92.6	
September	570	91.6	97.0	80.9	92.0	65.4	81.0	
Four Months	2226	89.6	95.6	77.2	88.0	65.2	82.2	
January	267	91.0	95.1	90.8	96.3	73.8	88.0	Non-Spread
April	288	95.2	98.3	94.4	96.5	82.6	95.1	
July	133	96.2	97.7	82.8	90.3	75.2	85.7	
September	259	93.0	97.0	93.4	97.0	78.8	90.7	
Four Months	947	93.6	96.9	91.1	95.7	78.0	90.6	

6.0 HARDWARE IMPLEMENTATION - ARTIST

The ARTIST (Automatic Real Time Ionogram Scaler with True height calculation) is an 8086 microprocessor based data cruncher which is contained in a 19" rack mountable chassis. The required high processing speed is achieved through the use of the 8087 arithmetic chip. The ARTIST has 500K of random access memory and 2 Mbyte of floppy disk storage. FORTRAN 77 is used as source language. At the present time, Digisonde 128PS ionograms are read from magnetic tape (9 tracks, 1600 bytes/inch) and processed to produce the traces, parameters and electron density profiles as discussed in the previous sections. Data transfer from the Digisonde 256 uses DMA techniques. To interface the ARTIST to the Digisonde 128PS requires some hardware/ software modifications. Data records from the DGS 128PS will be accepted by the ARTIST via an I/O port.

7.0 REFERENCES

Bibl, K. and B.W. Reinisch (1978), "The universal digital ionosonde," Radio Sci., 13, (13), 519-530.

Doupnik, J.R. and E.R. Schmerling (1965), "The reduction of ionograms from the bottomside and topside," J. Atmos. Terr. Phys., 27, 917-941.

Huang, X. and B.W. Reinisch (1982), "Automatic calculation of electron density profiles from digital ionograms. 2. True height inversion of topside ionograms with the profile-fitting method," Radio Sci., 17, (4), 837-844.

King, G.A.M. (1962), The Night E-layer, in "Ionospheric Sporadic E" (E.K. Smith and S. Matsushita, eds.).

Reinisch, B.W. and X. Huang (1982), "Automatic calculation of electron density profiles from digital ionograms. 1. Automatic O and X trace identification for topside ionograms," Radio Sci., 17, (2), 421-434.

Reinisch, B.W. and X. Huang, "Automatic calculation of electron density profiles from digital ionograms. 3. Processing of bottomside ionograms," to be published in Radio Science.

Reinisch, B.W., H.E. Moses and J.S. Tang (1981), "Automatic Processing of Digital Ionograms and Full Wave Solutions for the Profile Inversion Problem," AFGL-TR-82-0014, ULRF-417/CAR, Final Report.

Titheridge, J.E. (1967), "Direct manual calculation of ionospheric parameters using a single-polynomial analysis," Radio Sci., 2, (10), 1237-1253.

"U.R.S.I. Handbook of Ionogram Interpretation and Reduction," Second Edition, ed. W.R. Piggott and K. Rawer, pub. World Data Center A, Boulder, Colorado, 1972.

APPENDIX A

PREPRINT OF PAPER SUBMITTED TO RADIO SCIENCE, JULY 1982

AUTOMATIC CALCULATION OF ELECTRON DENSITY PROFILES FROM DIGITAL IONOGRAMS

3. PROCESSING OF BOTTOMSIDE IONOGRAMS

Bodo W. Reinisch and Huang Xueqin*

University of Lowell Center for Atmospheric Research

Lowell, Massachusetts 01854

ABSTRACT

Automatic scaling of bottomside Digisonde ionograms gives the E and F region echo traces with high accuracy. Polarization and incidence angle information in the ionogram enable the extraction of the vertical, ordinary polarization echo trace from quiet as well as disturbed ionograms. The scaling algorithm is tested with Digisonde ionograms from Goose Bay, Labrador, which show spread F about 50% of the time. Despite these disturbed conditions foF2 is determined within one-half megahertz for 475 ionograms out of 577 during January 1980. A profile inversion algorithm calculates the electron density profile from the autoscaled h'(f) points. Parabolic profile shapes are assumed for the E-region and the valley between E and F-layer. The F-layer is approximated by a single sum of Chebyshev polynomials, and the entire profile is described by a set of 13 numerical values. The CPU time required for ionogram scaling and electron density profile calculation is 14 seconds on a Cyber 71 computer. In addition to the profile the program outputs all relevant ionogram parameters: critical frequencies, minimum virtual heights, frequency and range spread, average echo amplitudes and Doppler shifts.

*On leave from Research Institute of Radiowave Propagation, Xinxiang, Henan, China.

1. INTRODUCTION

Automatic scaling of vertical ionograms from the many ground-based ionosondes has long been a desirable goal. Only nowadays when advanced digital sounders like the Digisonde [Bibl and Reinisch, 1978] are available can this goal be reached. Development of adequate sounding techniques was the unconditional prerequisite for the formation of successful algorithms to automatically scale the E and F region echo traces in a vertical ionogram. In the past, some very impressive results were occasionally shown where autoscaling methods were applied to a few selected ionograms. What we want to show in this paper is an autoscaling algorithm that works with quiet and disturbed ionograms, and that vertical electron density profiles can routinely be determined at each modern Digisonde station. Ionograms from the Goose Bay Ionospheric Observatory (64.6N geomagnetic) of the Air Force Geophysics Laboratory form the data base of the study. These ionograms display a large variety of features: quiet and disturbed daytime recordings, heavy spread F during the night, the mid-latitude trough moving over the station, fast variation of the ionospheric parameters and frequent absorption events.

The typical features of a quiet daytime ionogram are shown in Figure 1: a weak E-trace, transition to the F-trace, splitting in O and X polarization echoes and double echoes. The lower part of the figure shows the amplitude ionogram, the upper part the so-called status ionogram, explaining the echo type for each amplitude pixel. The ionogram, distinguishes O and X echoes, vertical and off-vertical echoes as well as positive and negative Doppler shifts. The scaling algorithm extracts the vertical ordinary echo trace from which the electron density profile is calculated.

Section 2 describes the algorithm for the autoscaling of the bottomside Digisonde ionograms, and Section 3 explains the profile inversion technique for autoscaled data. Reference is frequently made to the two earlier papers in this sequence of three [Reinisch and Huang, 1982 and Huang and Reinisch, 1982], which are cited as Part 1 and Part 2.

2. AUTOSCALING OF DIGITAL BOTTOMSIDE IONOGRAMS

It has long been recognized that a network of bottomside ionosondes provides a wealth of ionospheric information valuable for research and communication. The tedious effort involved in scaling and evaluating the conventional analog ionograms has been a consistent deterrent to widespread use of ionogram data. In recent years digital ionosondes became available and a serious effort began, to find ways to automatically scale the ionograms. At that point it seemed tempting to no longer generate complete ionograms but to reduce the soundings to a few frequencies centered around the predicted critical frequencies of the E, F1 and F2 region and to merely retrieve a few critical parameters. The complexity of disturbed ionograms especially in the auroral and equatorial regions makes this approach all but impossible. Even a complete digital ionogram which merely records amplitudes as function of range and frequency (lower part of Figure 1) is inadequate for autoscaling. The amplitude information must be complemented by polarization flagging, and the distinction between vertical and off-vertical echoes. The Digisonde at Goose Bay routinely records these multiparameter ionograms on magnetic tape. This made it possible to develop ionogram processing software at a main frame computer (Cyber 71 or CDC 6600) and test its performance by applying the software to a large number of ionograms.

Signal-to-Noise Enhancement

The location of a station determines the noise level in the ionograms, since it is generally man-made interference rather than white thermal or atmospheric noise which obscures the echo traces. Although the phase coherent spectral integration in the Digisonde, which transmits high-frequency-phase coded pulse signals, significantly reduces unwanted signals, strong interferers still contaminate the ionograms in form of discrete noise lines. The typical signature of interference is a fairly constant distribution of amplitudes over the range bins, while the echo signals occupy only two to three range bins. Because of the discrete nature of the man-made interference the data for each ionogram frequency is processed individually. The most probable amplitude found over all range bins for a given frequency is used to set the noise threshold. During severe spread F conditions, the most probable amplitude could be the signal level, setting too high a threshold. To avoid this problem, two probability curves are formed, one for the lower 64 and one for the higher 64 range bins. (The Digisonde 128PS uses 128 range bins.) The distribution that peaks at a lower amplitude sets the threshold [Reinisch and Smith, 1976].

E-Region Trace

The task of determining the h'(f) function for the vertical echoes with ordinary polarization is divided into the two parts of finding the E-trace and the F-trace. Since one can devise a generic function to approximate the normal E-trace, which is impossible for the F-trace, it is a relatively easy task to find the E-trace. Assuming a parabolic electron density distribution in the E-region [Bradley and Dudeney, 1973]

$$N(z) = N_E \{1 - (\frac{z-z_E}{y_E})^2\} \quad (1)$$

one can calculate the virtual height function h'(f):

$$h'(f) = \int_0^{z(f)} \mu' \, dz; \quad (2)$$

N(z) = electron density at height z

N_E = electron density at height z_E, the peak of the E-layer

y_E = half thickness of the parabolic profile

f = transmitted frequency

μ' = group index of refraction

f_E = foE = 9.0 $\sqrt{N_E}$ MKS units, critical frequency of E-layer.

Neglecting the geomagnetic field it is easy to analytically calculate the virtual height as [Davies, 1965, p. 135]:

$$h'(f) = z_E - y_E + \frac{1}{2} y_E \frac{f}{f_E} \ln \frac{f_E+f}{f_E-f} . \quad (3)$$

A simple search algorithm determines the three unknown parameters f_E, z_E and y_E. Each h'(f) function defined by equation (3) traces out a sequence of amplitude pixels in the ionogram. The sum along the trace of all amplitudes with ordinary and vertical identification is the measure for the quality of the fit. The parameters f_E, z_E and y_E are varied until the maximum sum is found. Actually, the amplitude sum is always normalized by dividing it by the number of frequency increments, and this average amplitude is optimized. The optimum trace follows the peaks the echo pulses. The entire trace is, therefore, lowered until the average amplitude per frequency is reduced by 6 dB. This lowered trace follows the leading edge of the echo pulses, and can directly be compared with the manually scaled h'(f) trace.

Fortunately, the range of the parameter values is rather small. The critical frequency f_E can be predicted within ±0.3 MHz, i.e. only seven f_E values have to be tested for ionograms with 100 kHz frequency increments. The half thickness y_E is varied from 10 to 40 km in 5 km steps, resulting in seven values. The height of the layer peak, z_E, is varied from 95 to 150 km, meaning 12 values in case of 5 km range increments. The total number of h'(f) functions to be tested is 7 × 7 × 12 = 588. The status identification of the echo amplitude pixels allows this simple fitting procedure, otherwise X-echoes would cause severe errors. The method works very reliably even under disturbed conditions. In Figures 2 and 3 the letters O, X and B indicate vertical ordinary and extraordinary echoes and oblique echoes, respectively. The autoscaling (dark circles) properly follows the O-echoes.

Special provisions for high latitude stations allow the detection of particle ionization in the E-region, often called night E [King, 1962]. As soon as the predicted foE value goes below 2.5 MHz, the program tests for critical frequencies of up to 6 MHz or the center (see below) of the F-trace, whatever is lower in frequency. Figure 3 is an example of a night E condition in Goose Bay with foE = 2.6 MHz at 20:19 local time. Ordinary echo traces beyond foE are identified as Es (foEs = 4.0 MHz in Figure 2 and 3.1 MHz in Figure 3).

F-Region Trace

Part 1 discussed the methods of autoscaling the F-region echoes for topside ionograms, and very similar methods apply to the bottomside soundings. The large variations in height and shape of the F-region traces, together with the occurrence of multiple echoes and spread F make it impossible to use a simple curve fitting procedure for the entire

F-trace. During disturbed ionospheric conditions, it is often difficult to identify the main overhead echo trace. In Goose Bay this is especially true when the mid-latitude F-region trough [Sharp, 1966; Bowman, 1969] moves over the station. The direction finding capability of the Digisonde identifies the bulk of the oblique echoes, but angular resolution and sidelobes of the antenna array pattern can cause erroneous identifications. In analogy to visual inspection, the automatic trace identification starts by finding the center of the F-trace, i.e. the region where the change of h' with frequency is small and the echo amplitude is strong. A first rough trace, called the baseline, is then constructed by sliding a searching window (5 frequencies × 35 range bins) frequency-by-frequency from the trace center toward higher and lower frequencies. In an effort to minimize the required CPU time, the program uses selected data points, called first local maxima (FLM). For each frequency the position of the first (in the direction of increasing range) amplitude maximum of an O-echo between two zero amplitudes is defined as an FLM. The number of FLM's per frequency is not limited. Each FLM is checked whether it is a double or triple echo by comparing its amplitude with the pixel at half or two-thirds the range. If the FLM is smaller in amplitude, it is deleted.

The frequency-by-frequency searching process defines a rough trace close to the leading edge of the pulse and is able to successfully trace the F1/F2 transitions, but it also produces some undesired h' discontinuities when man-made interferers distort the echo pulses at certain frequencies. Also, in the F2 cusp region, the baseline is generally a poor representation (Figure 3) of the ordinary F-trace when spread F and external interference are present.

Since the ordinary vertical echoes are identified in the Digisonde ionograms, piecewise smoothing of the data

is possible, in contrast to the situation described in Part 1 for the topside ionograms. A six-point smoothing method based on the signal amplitudes is described in detail in an unpublished report [Reinisch et al, 1982]. For frequencies below the cusp region the smoothed baseline runs just below the peaks of the echo pulses. The fast rise in h' at the F2 cusp and the frequent occurrence of spread F require a special fitting procedure for the trace near foF2.

Hyperbolic Trace Fitting at the F2 Cusp

A polynomial or a suitable rational function can describe the F2 cusp with reasonable accuracy. The simple hyperbolic function

$$h'_x = r + \frac{1}{a+bf} \qquad a > 0,\ b < 0 \tag{4}$$

has a pole at f = - a/b and is, therefore, well suited to fit the trace near the critical frequency. The coefficients r, a and b are determined in such a way that the h'-function follows the pixels with the maximum amplitudes, assuring that a reasonable cusp will be defined even in the presence of spread F. Frequently the O-trace near foF2 is not visible on the ionograms because of ionospheric conditions or high interference, while the X-trace is clearly developed. The reliability of the autoscaling is therefore largely improved if an O and an X hyperbola are simultaneously fitted to the polarization tagged amplitude data. If equation (4) is the X-hyperbola, the O-hyperbola is given by

$$h'_o = r + \frac{1}{a+bf^*} \tag{5}$$

with $f^* = f + \frac{1}{2} fH$, where the gyrofrequency fH is evaluated for 300 km altitude. The two hyperbolas (4) and (5) are simply offset by half the gyrofrequency, and they are posi-

tioned on the ionograms such as to maximize the sum of the O and X amplitudes in narrow stripes around the O and X-hyperbolas, as shown in Figure 4. For each hyperbola point the amplitudes are summed downward to the height of the preceding frequency. This method forces the hyperbola to the inner edge of the trace cup. The computer printout of the ionogram in Figure 4 does not show the signal amplitudes, but instead the polarization tags O and X for the vertical echoes, and the letter B for the oblique echoes. Only O-signals contribute to the O-hyperbola's amplitude summation, and X-signals to the X-hyperbola's. The hyperbolic traces for the ionogram in Figure 4 are marked by heavy dots (O-trace) and X's (X-trace). The hyperbolic section of the trace ends where the O-hyperbola intersects the baseline (3.3 MHz), and the baseline then defines the trace toward lower frequencies.

An adequate set of hyperbolas in the neighborhood of the cusp region must be tried to find one that simulates the F cusp. Using the baseline points as a guide the method of min-max rational functions [Scheid, 1968, p. 289] fits hyperbolas to subsets of three points. Starting at the high frequency end of the baseline, a hyperbola is fitted to the last three baseline points by minimizing the distance x from the hyperbola (see Figure 5). The range deviations of the three points (f_i, h_i') from the curve are

$$h_i' - \{r + \frac{1}{a + bf_i}\} = (-1)^{i-1} x \qquad i = 1, 2, 3. \tag{6}$$

These equations can be written in the form (deleting the primes on the heights):

$$(h_1 - r - x)a + (h_1 - r - x)f_1 b - 1 = 0 \tag{7}$$

$$(h_2 - r + x)a + (h_2 - r + x)f_2 b - 1 = 0 \tag{8}$$

$$(h_3 - r - x)a + (h_3 - r - x)f_3 b - 1 = 0 \tag{9}$$

Eliminating a and b leads to a quadratic equation for the determination of x

$$\begin{vmatrix} h_1 - r - x & (h_1 - r - x) f_1 & 1 \\ h_2 - r + x & (h_2 - r + x) f_2 & 1 \\ h_3 - r - x & (h_3 - r - x) f_3 & 1 \end{vmatrix} = 0 \qquad (10)$$

or,

$$x = - \frac{B}{2A} \left(1 - \sqrt{1 - \frac{4AC}{B^2}}\right) \qquad (11)$$

where

$$A = 2 (f_1 - f_3) \qquad (12)$$

$$B = B_0 + Ar \qquad (13)$$

$$C = C_0 - C_1 r \qquad (14)$$

$$B_0 = - f_1(h_3+2h_1-h_2) - f_2(h_3-h_1) - f_3(h_2-2h_3-h_1) \qquad (15)$$

$$C_0 = f_1h_1(h_3-h_2) + f_2h_2(h_1-h_3) + f_3h_3(h_2-h_1) \qquad (16)$$

$$C_1 = f_1(h_3-h_2) + f_2(h_1-h_3) + f_3(h_2-h_1). \qquad (17)$$

The coefficients B and C are functions of the base height r, which is unknown. Inspection of equation (11) shows that $|x|$ will be a minimum if $4AC/B^2 = 0$. This may not be possible to achieve, but one can find the minimum value of $|AC/B^2|$, by setting the derivative with respect to r equal to zero:

$$\frac{d}{dr} \left(\frac{AC}{B^2}\right) = 0 \qquad (18)$$

resulting in

$$r = \frac{C_1 B_0 + 2 AC_0}{AC_1} \qquad (19)$$

Once r and x are calculated from (19) and (11) the coefficients a and b, specifying the X-hyperbola, can be found. The corresponding O-hyperbola is determined by simply replacing f by f*. Finally the O and X sums are determined.

It is of course unlikely that the hyperbolas fitted to the last three points (highest frequency) of the baseline will be a good approximation for the traces in the cusp region. The process is repeated for the next three points and so on, down to frequencies at the center window. The same process is then applied to triple points spaced by two frequencies and by three frequencies. By numbering the baseline data points from 1 to N, one can write the triple point sets to which hyperbolas are fitted in the following way:

GROUP 1			GROUP 2			GROUP 3		
P_1	P_2	P_3	P_1	P_3	P_5	P_1	P_4	P_7
P_2	P_3	P_4	P_2	P_4	P_6	P_2	P_5	P_8
-	-	-	-	-	-	-	-	-
-	-	-	-	-	-	-	-	-
P_{N-2}	P_{N-1}	P_N	P_{N-4}	P_{N-2}	P_N	P_{N-6}	P_{N-3}	P_N

The total number of trial hyperbolas is 3N-12. From these hyperbolas the one with the maximum O and X amplitude sum is selected for the trace representation. Combining the O-hyperbola with the smoothed baseline results in a preliminary trace for the O-polarization echoes. Lowering the entire curve to the leading edge of the echo pulses gives the final F-trace. Figures 6 and 7 illustrate the performance of the scaling algorithm for quiet and disturbed conditions. Figure 7 shows the F-trace before it had been lowered.

Parameter Extraction

At the present time, the program determines the following ionospheric parameters: foF2, foF1, fminF, MUF (3000), M(3000), range spread F, frequency spread F, h'F, foE, foEs, range spread E, frequency spread E, h'E, h'Es (parameters are defined in the U.R.S.I. Handbook of Ionogram Interpretation and Reduction, Second Edition, November 1972, by W. R. Piggott and K. Rawer, World Data Center A, Report UAG-23). In addition, averaged echo amplitude values are given for each megahertz, normalized to a reflection height of 100 km. The Doppler signatures of the echoes are also saved for further analysis. Statistical evaluation of these autoscaled parameters will be discussed in another paper, but to illustrate the performance level of the scaling algorithm the comparison between manual and autoscaled foF2 values is given in Figure 8. The dashed curves are the error distribution for 577 hourly ionograms from Goose Bay, January 1980; 82% of these ionograms have an error of less than 0.5 MHz. The solid curves include only the 256 ionograms without spread F. The difference between the solid and the dashed curve is acceptably small, showing that the algorithm performs reasonably well also in the presence of spread F. as demonstrated in Figure 7. The autoscaling of the F-trace during this trough affected ionograms is remarkably accurate. The ionograms show several cusps and the one selected by the program is the vertical echo trace with the strongest amplitudes. Differences in interpretation in this type ionogram are the main reason for foF2 errors of 1 to 2 MHz.

3. CALCULATING THE VERTICAL ELECTRON DENSITY PROFILE

Part 2 discussed an efficient method of inverting the h'(f) trace into the vertical electron density profile,

using the autoscaled h'(f) data points as input. The profile is described by a sum of Chebyshev polynomials the coefficients of which are optimized in a least-squares sense to best reproduce the measured h'(f) trace. This profile-fitting method is well suited for autoscaled data and describes a monotonic profile with a single polynomial. The bottomside profile may have an ionization valley between E and F region and the polynomial ansatz must be expanded. Figure 9 shows a reasonable model of a vertical electron density distribution, which is convenient for calculational purposes: up to the height z_1 the profile is described by the E-region parabola defined by f_E, y_E and z_E, the F-region above z_2 is represented by a single polynomial (as in the case of the topside profile), and the valley around z_v is represented by another parabola which smoothly connects to the E-parabola at z_1 and the F-profile at z_2. While this valley may not precisely describe the actual profile in this height region it allows for a better profile presentation than the assumption of a monotonic distribution. A reasonable D region profile could be added, modifying the E-parabola for $f \to 0$.

Model Parameters

The E-region parabola was already determined in the scaling algorithm, so f_E, z_E and y_E are known. If the profile between z_1 and z_2 were known one could calculate the F-profile with the profile-fitting technique, since $z_2 = z_E + w$ could be derived. Using the expressions derived in Part 2 one can write for the contribution of the F-region to the vertical height at frequency

$f_k > f_E$:

$$\Delta h'_F(f_k) = \sum_{i=0}^{I} A_i \, S_{ik}, \qquad I \leq 7. \tag{20}$$

The A_i define the F-profile ($z_2 \leq z \leq z_F$):

$$z = A_{I+1} + \sqrt{g} \sum_{i=0}^{I} A_i \, T_i^*(g) \tag{21}$$

with

$$g = \frac{\ln (fN/f_F)}{\ln (f_E/f_F)} \, . \tag{22}$$

The T_i^* are the shifted Chebyshev polynomials (Part 1; Snyder, 1966, p. 20). The S_{ik} were given as

$$S_{ik} = \frac{f_k^2 - f_E^2}{2 \ln (f_E/f_F)} \int_0^1 \frac{\mu' t}{f_N^2 \sqrt{g}} \{T_i^*(g) + 2 \, g \, \frac{d}{dg} \, T_i^*(g)\} \, dt \tag{23}$$

with

$$t^2 = \frac{f_k^2 - fN^2}{f_k^2 - f_E^2} \text{ or } fN^2 = f_k^2 - t^2 \, (f_k^2 - f_E^2). \tag{24}$$

At the F-layer peak g = 0 and

$$z_F = A_{I+1}; \tag{25}$$

at height z_2 the g value is 1, and $T_i^*(1) = 1$, so

$$z_2 = A_{I+1} + \sum_{i=0}^{I} A_i, \tag{26}$$

or

$$z_F - z_2 = - \sum_{i=0}^{I} A_i. \tag{27}$$

All these expressions were derived in Part 2 for the topside profile; the plasma frequency at the satellite, fN_S, is replaced for the bottomside by f_E. Only the ordinary echo trace is considered, as is usually done for the bottomside ionosphere. Dependence on the height variation of the

geomagnetic field is less critical and it suffices to calculate the S_{ik} for constant gyrofrequency fH and dip angle θ at a height of 300 km. For given f_E and f_F the S_{ik} can be calculated for all scaled frequencies f_k. The group refractive index μ' for the ordinary polarization was given in the Appendix of Part 2.

The virtual height of an F-echo at frequency f_k is composed of E, valley and F-region contributions (see Appendix):

$$h' = \frac{c}{2} t = \Delta h'_E + \Delta h'_V + \Delta h'_F \qquad (28)$$

(c = speed of light in free space, t = observed group travel time).

The F profile is determined by minimizing the square error of the differences between the observed virtual F heights h'_k and the values obtained from (28):

$$\varepsilon = \sum_{k=1}^{K'} [h'_k - (\Delta h'_{Ek} + \Delta h'_{Vk} + \sum_{i=0}^{I} A_i S_{ik})]^2. \qquad (29)$$

h'_k is measured and $\Delta h'_{Ek}$ can be calculated (see equation A2). The square sum is taken only over the data points of the lower F-region (K' is the frequency index that is associated with the minimum virtual height). This part of the F-trace is more sensitive to the valley shape than the trace at higher frequencies. It is shown in the Appendix that the valley contribution depends on the valley width w and the slope B at z_2. In an iterative procedure w, B, and the A_i coefficients are determined such as to minimize the error ε in (29) (see the Appendix and also Part 2 for the calculation of A_i). The requirement of smooth transitions between the three profile functions gives the valley parameters z_1, z_V, y_V, $z_2 = z_E + w$ and f_V. The F-profile is specified by the nine (or less) coefficients A_0, A_1, . . ., A_{I+1}. The order I of the polynomial expansion (21) is auto-

matically reduced from its maximum value of 7 if the profile shape allows it (Part 2). For archiving or remote data transfer one should allocate space for sixteen numerical values which give a detailed description of the entire electron density profile: f_E, z_E, y_E, f_V, z_V, y_V, f_F, A_0, A_1, . . ., A_{I+1}.

Discussion of Electron Density Profiles

It should be noted that the calculations for the E and valley regions neglected the geomagnetic field. In principle, this would not be necessary, but it simplifies the calculations without introducing significant errors, considering the limited accuracy of the autoscaling.

The automatic vertical electron density profiles for the ionograms in Figures 2, 3 and 6 are shown in these figures. As a measure of the quality of the automatic profile technique, the auto profiles are compared with the corresponding "manual" profiles, obtained by manually scaling the ionogram and applying the conventional lamination method for the true height inversion. These comparisons are shown in Figures 10, 11, and 12. The daytime profiles in Figure 10 show variances of about 10 km, but in general the agreement between auto and manual profile is very good. The third curve is calculated by applying the lamination inversion method to the autoscaled data. This curve is very close to the auto profile indicating the validity of the profile-fitting method. Similar good agreement is shown by the night profiles in Figure 11 for the disturbed ionogram in Figure 3. The day profile in Figure 12 has an ionization valley between the E and F layer, which of course cannot be determined by the standard lamination technique. The valley minimum is located at f_V = 2.1 MHz and z_v = 139 km; the width of the valley is 36 km.

For comparison with the International Reference Ionosphere IRI [Rawer et al, 1978 and 1981] it might be desirable to express the profile as a sum of Epstein-step-functions [Booker, 1977]. This, however, need not be done at the ionosonde site. The automatic profile technique described in this paper is tailored for real time application in a microprocessor based Digisonde chassis which will be field tested within the next few months.

4. CONCLUSION

Ground based digital ionograms with polarization and incidence angle identifications can be successfully auto-scaled for quiet and for disturbed ionospheric conditions, and the corresponding vertical electron density profiles can be calculated. By installing automatic real time ionogram scaler with all modern digital ionosondes could provide an always up-to-date global ionospheric model, assuming a sufficient number of these stations.

ACKNOWLEDGEMENT

This work was in part supported by Air Force contracts F19628-80-C-0113 and F19628-80-C-0064. The authors wish to thank J. Tang and R. Gamache for their contributions in developing the algorithms and writing the computer program.

REFERENCES

Bibl, K. and B. W. Reinisch (1978), The universal digital ionosonde, Radio Sci., 13 (13), 519-530.

Booker, H. G. (1977), Fitting of multiregion ionospheric profiles of electron density by a single analytic function of height, J. Atmos. Terr. Phys., 39, 613-623.

Bowman, G. G. (1969), Ionization trough below the F2-layer maximum, Planet. and Space Sci., 17, 777.

Bradley, P. A. and J. R. Dudeney (1973), A simple model of the vertical distribution of electron concentration in the ionosphere, J. Atmos. Terr. Phys., 35, 2131.

Davis, K. (1966), Ionospheric Radio Propagation, Dover Publications, New York, 470 pages.

King, G. A. M. (1962), The Night E-Layer, in "Ionospheric Sporadic E" (E. K. Smith and S. Matsushita, eds.).

Muldrew, D. B. (1965), F-layer ionization troughs deduced from Alouette data, JGR, 70, 2635.

Rawer, K., D. Bilitza and S. Ramakrishnan (1978), Goals and status of the International Reference Ionosphere, Rev. of Geophys. and Space Phys., 16 (2), 177-181.

Rawer, K. (1981), International Reference Ionosphere - IRI 1979, (J. V. Lincoln and R. O. Conkright, eds.), World Data Center A for Solar-Terrestrial Physics, Report UAG-82.

Reinisch, B. W., H. E. Moses and J. S. Tang (1982), Automatic processing of digital ionograms and full wave solutions for the profile inversion problem, Final Report AFGL-TR-82-0014, Univ. of Lowell Center for Atmos. Res., Lowell, Mass.

Reinisch, B. W. and S. Smith (1976), Geomonitor, digital real time processor for geophysical data, Final Report AFGL-TR-76-0292, Univ. of Lowell Center for Atmos. Res., Lowell, Mass.

Reinisch, B. W. and H. Xueqin (1982), Automatic calculation of electron density profiles from digital ionograms. 1. Automatic O and X trace identification for topside ionograms, Radio Sci., 17 (2), 421-434.

Reinisch, B. W. and H. Xueqin (1982), Automatic calculation of electron density profiles from digital ionograms. 2. True height inversion of topside ionograms with the profile-fitting method, Radio Sci.

Sharp, G. W. (1966), Mid-latitude trough below the F2-layer maximum, Planet. and Space Sci., 17, 777, 1345.

APPENDIX

Parabolic E and valley regions:

$$fN^2 = \begin{cases} 0 & z < z_E - y \\ f_E^2 \left[1 - \left(\frac{z-z_E}{y_E}\right)^2\right] & z_E - y \le z \le z_1 \\ f_V^2 \left[1 + \left(\frac{z-z_V}{y_V}\right)^2\right] & z_1 \le z \le z_2. \end{cases} \quad \text{(A1)}$$

Virtual height contributions for $f_k > f_E$:

$$\Delta h'_E = z_E - y_E + \frac{1}{2} y_E \frac{f_k}{f_E} \ln \frac{f_k + f_E}{f_k - f_E}, \quad z_E - y_E \le z \le z_E \quad \text{(A2)}$$

$$\Delta h'_{V1} = f_k \sqrt{Y} \ln \frac{\sqrt{\frac{DY}{Y+4B^2D}} + \sqrt{f_k^2 - f_E^2 + \frac{DY}{Y+4B^2D}}}{\sqrt{f_k^2 - f_E^2}}, \quad z_E \le z \le z_1. \quad \text{(A3)}$$

For $z_1 < z < z_2$:

$$\Delta h'_{V2} = 2f_k B \sqrt{D} \left[\sin^{-1} \frac{\sqrt{D}}{\sqrt{f_k^2 - f_E^2 + D}} + \sin^{-1} \frac{2BD}{\sqrt{(y+4B^2D)(f_k^2 - f_E^2 + D)}}\right] \quad \text{(A4)}$$

$$Y = \frac{y_E^2}{f_E^2}, \quad D = f_E^2 - f_V^2 = \frac{w^2}{Y + 4wB}, \quad w = z_2 - z_E$$

$$B^{-1} = \left.\frac{dfN^2}{dz}\right|_{z=z_2} = \frac{d}{dz} f_V^2 \left[1 + \left(\frac{z-z_V}{y_V}\right)^2\right] = 2 \frac{f_V^2}{y_V^2} (z-z_v), \quad \text{(A5)}$$

where w is a measure of the valley width and B defines the slope at z_2 where the valley parabola joins the F-profile. This means that B must also equal the slope of the F-profile at z_2:

$$B = \frac{1}{4\, f_E^2\, \ell n\, (f_E/f_F)} \sum_{i=0}^{I} A_i \left[1 + 2 \left(\frac{d}{dg}\, T_i^*\right)_{g=1}\right]. \qquad (A6)$$

The total contribution of the valley region $z_E \leq z \leq z_2$ is

$$\Delta h'_V = \Delta h'_{V1} + \Delta h'_{V2} = \Delta h'_V\, (f_k, f_E, y_E, w, B) \qquad (A7)$$

where w and B are the only two unknowns. Setting w = 0 and B = 0 one can calculate a set of initial coefficients A_i using the least-squares error method:

$$\epsilon = \sum_{k=1}^{K} \left[h'_k - (\Delta h'_{Ek} + \Delta h'_{Vk} + \sum_{i=0}^{I} A_i\, S_{ik})\right]^2 \qquad (A8)$$

where K is the number of F-trace data points. Minimizing this error means solving the set of I+1 equations for the A_i:

$$\sum_{k=1}^{K} (h'_k - \Delta h'_{Ek} - \Delta h'_{Vk})\, S_{jk} = \sum_{i=0}^{I} A_i\, Q_{ij},\ j = 0, 111, I \qquad (A9)$$

with

$$Q_{ij} = \sum_{k=1}^{K} S_{ik}\, S_{jk} \qquad i, j = 0, 1, 111, I. \qquad (A10)$$

At frequency f_E, g = 1 and $z = z_2$ and the equation for z

$$z = A_{I+1} + \sqrt{g} \sum_{i=0}^{I} A_i\, T_i^*(g) \qquad (A11)$$

reduces to

$$z_2 = A_{I+1} + \sum_{i=0}^{I} A_i$$

since $T_i^*(1) \equiv 1$.

This determines the last coefficient:

$$A_{I+1} = z_E + w - \sum_{i=0}^{I} A_i \qquad \text{(A12)}$$

The slope B is now calculated from (A6) and a new set of coefficients A_i is determined. In this iteration loop for B only the part of the F-trace between f_E and $f_{K'}$ is used, where h'F has its minimum at $f_{K'}$. The process is then repeated for w = 1 km, 2 km, etc. The parameter pair w, B which has the smallest least-square error in equation (A8) is used to describe the valley profile and to calculate the final set of coefficients A_i for the F-profile.

The valley parameters z_1, z_V, f_V, y_V and z_2 are obtained from the smoothness requirements for the profile function at z_1 and z_2. At $z = z_2$:

$$f_E^2 = f_V^2 \left[1 + \left(\frac{z_2 - z_V}{y_V}\right)^2\right] \qquad \text{(A13)}$$

$$B = \left.\frac{dz}{d(fN^2)}\right|_{z=z_2} = \frac{y_V^2}{2(z_2 - z_V)\, f_V^2}. \qquad \text{(A14)}$$

This leads to:

$$y_V = 2\, B\, f_V \sqrt{D} \qquad \text{(A15)}$$

and

$$z_2 = z_V + 2BD. \qquad \text{(A16)}$$

The smoothness condition at $z = z_1$ requires that the quadratic equation

$$f_E^2 \left[1 - \left(\frac{z-z_E}{y_E}\right)^2\right] = f_V^2 \left[1 + \left(\frac{z-z_V}{y_V}\right)^2\right] \tag{A17}$$

has only one solution for z. This gives

$$z_1 = \frac{z_V\, Y + z_E \left(\frac{y_V}{f_V}\right)^2}{Y + \left(\frac{y_V}{f_V}\right)^2} \tag{A18}$$

and

$$z_V = z_E + \sqrt{D[Y + (y_V/f_V)^2]}. \tag{A19}$$

Substituting (A15):

$$z_1 = \frac{z_V\, Y + 4 z_E\, B^2 D}{Y + 4\, B^2 D} \tag{A20}$$

$$z_V = z_E + \sqrt{D[Y + 4B^2 D]}. \tag{A21}$$

The parameter D is a function of w and B; from (A16);

$$w \equiv z_2 - z_E = z_V - z_E + 2\, BD = \sqrt{D[Y+4\, B^2 D]} + 2BD \tag{A22}$$

or

$$D = \frac{w^2}{Y + 4wB}. \tag{A23}$$

The definition for the virtual height contributions for the valley is (neglecting the geomagnetic field):

$$\Delta h' = \int_{z_A}^{z_B} \mu'\, dz = \int_{z_A}^{z_B} \frac{dz}{\sqrt{1 - \frac{fN^2}{f^2}}}$$

$$\Delta h'_{V1} = \int_{z_E}^{z_1} \frac{dz}{\sqrt{1-\left(\frac{f_E}{f}\right)^2 \left[1-\left(\frac{z_E-z}{y_E}\right)^2\right]}}, \tag{A24}$$

$$\Delta h'_{V2} = \int_{z_1}^{z_2} \frac{dz}{\sqrt{1-\left(\frac{f_V}{f}\right)^2\left[1+\left(\frac{z-z_V}{y_V}\right)^2\right]}} \cdot \qquad \text{(A25)}$$

Figure 1 Digisonde Ionogram

Real time Digisonde 128PS ionogram with optically weighted font displaying signal amplitudes (bottom) in 4 dB increments and status (top). Sixteen level status indicates 3 incidence angles, O and X polarization and 4 Doppler frequencies.

Figure 2 Autoscaling for Relatively Quiet Ionogram

Normal E, sporadic E, F1 and F2 traces are accurately determined. The autoprofile shows only minute inflection at foF1 = 5.7 MHz.

Figure 3 Night E and Spread F

E and Es trace as well as the maximum F-trace are correctly identified. The baseline, labeled S, is shown for reference. The solid line is the auto-profile. The F region frequency spread is fxI - fxF2.

Figure 4 Amplitude Windows for Hyperbolas

The O (or X) amplitudes below each hyperbola point down to range of previous frequency are summed; for last frequency range window extends to upmost range bin.

Figure 5 Hyperbolic Fitting with Min-Max Method

Equal distance x of three points from hyperbola is minimized.

Figure 6 Autoscaling for Quiet Conditions

Small scaling errors occur at 8.8 MHz (O and X trace crossover) and at 5.0 MHz (reduced transmitter power). Weak E-trace is properly identified. Auto-profile shows valley between E and F.

Figure 7 Autoscaling During Trough Conditions

F-trace (before lowering) identifies the strongest vertical echo sequence while mid-latitude trough moves over Goose Bay.

Figure 8 Error Distribution of foF2

Relative deviation of auto foF2 from manually scaled values centers around zero. Inclusion of ionograms with spread F widens the distribution function only slightly.

Figure 9 Electron Density Profile Model

A parabolic valley smoothly joins the E-region parabola at z_1 and the F-region profile at z_2.

Figure 10 Daytime Profile for Quiet Conditions

Goose Bay 21 April 1980, 10:00 AST. Comparison of manual and automatic methods.

Figure 11 Nighttime Profile During Disturbed Conditions

Goose Bay 5 September 1980, 20:19 AST.

Figure 12 Daytime Profile with Ionization Valley

Goose Bay, 9 January 1980, 10:00 AST.
Lamination method cannot show the valley.

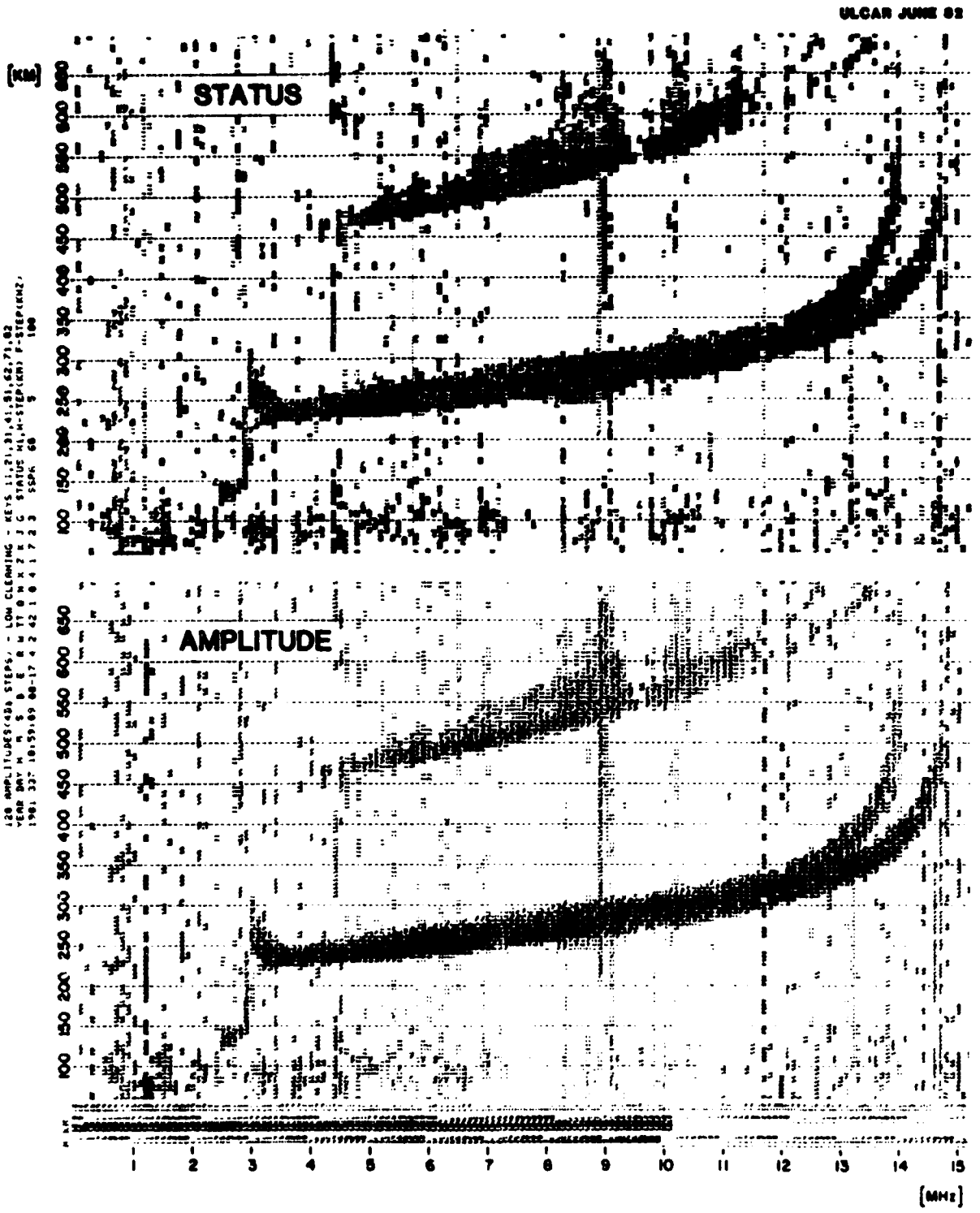

DIGISONDE IONOGRAM

GOOSE BAY 3 DEC 1981 11:00 AST

Figure 1

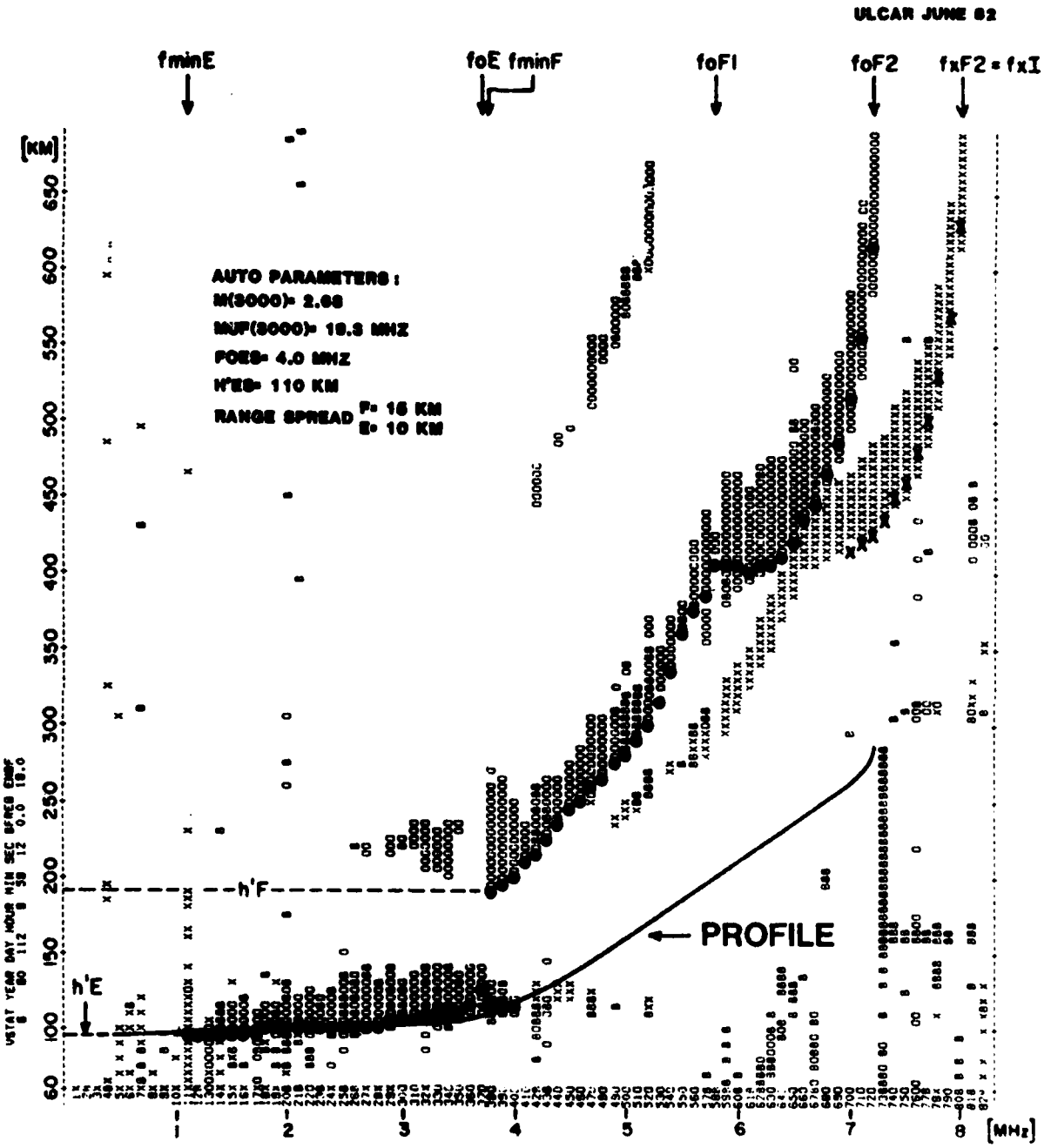

AUTOSCALING FOR RELATIVELY QUIET IONOGRAM

GOOSE BAY 21 APRIL 1980 10:00 AST

Figure 2

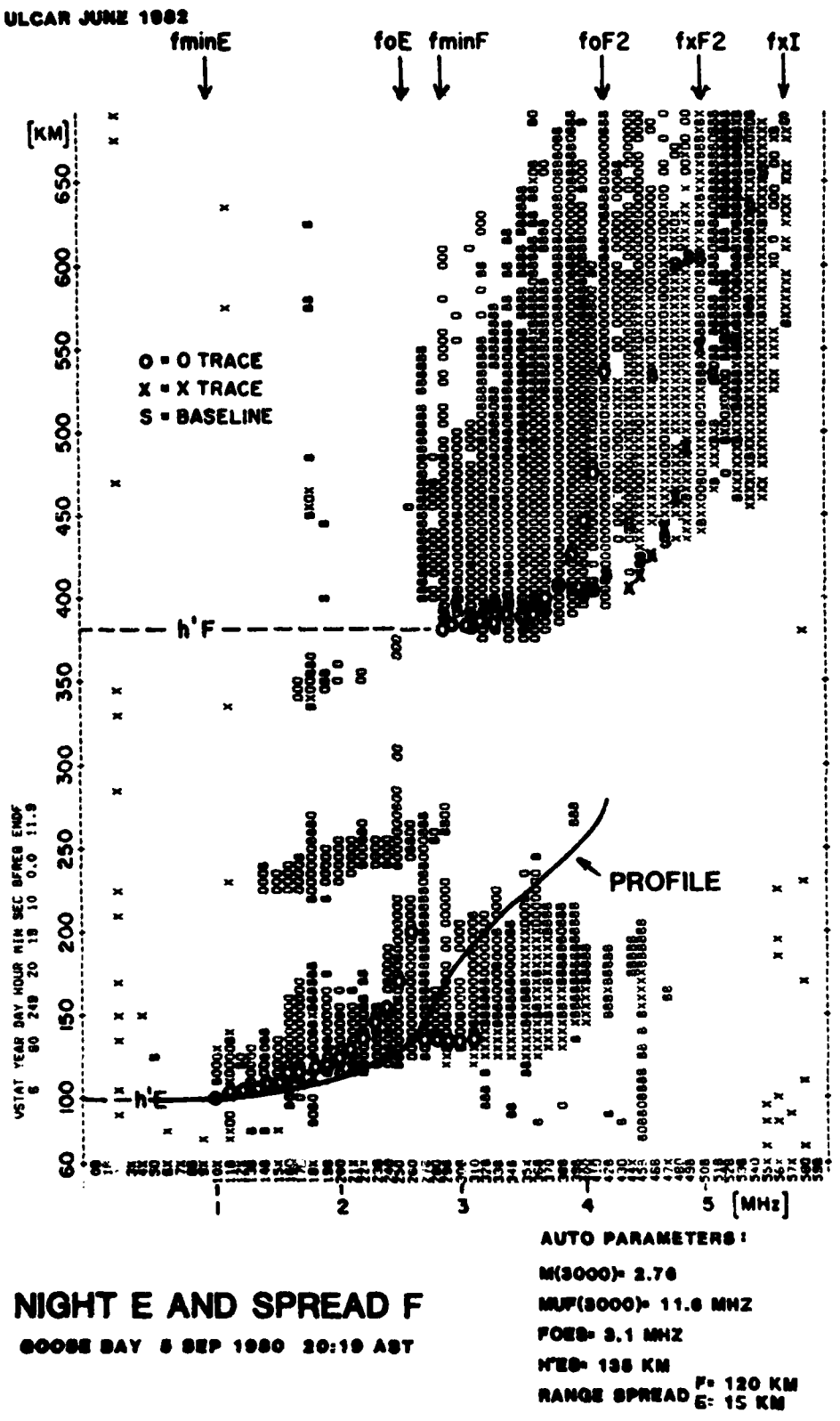
ULCAR JUNE 1982
fminE
foE
fminF
foF2
fxF2
fxI
[KM]
O = O TRACE
X = X TRACE
S = BASELINE
h'F
h'E
PROFILE
[MHz]
AUTO PARAMETERS:
M(3000)= 2.76
MUF(3000)= 11.8 MHZ
FOES= 3.1 MHZ
H'ES= 135 KM
RANGE SPREAD F= 120 KM
E= 15 KM
NIGHT E AND SPREAD F
GOOSE BAY 5 SEP 1980 20:19 AST

Figure 3

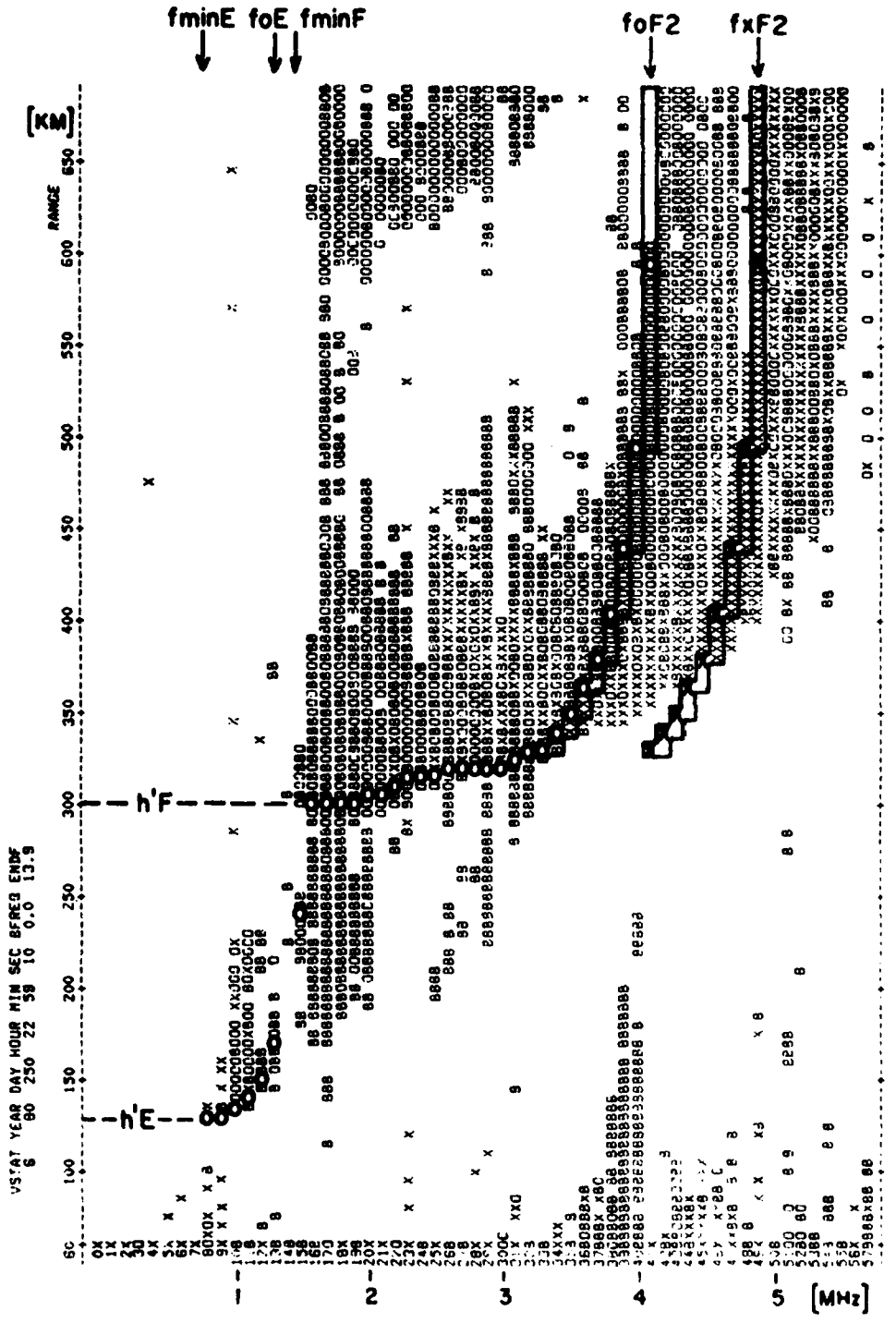

AMPLITUDE WINDOWS FOR HYPERBOLAS

GOOSE BAY 6 SEP 1980 23:00 AST

Figure 4

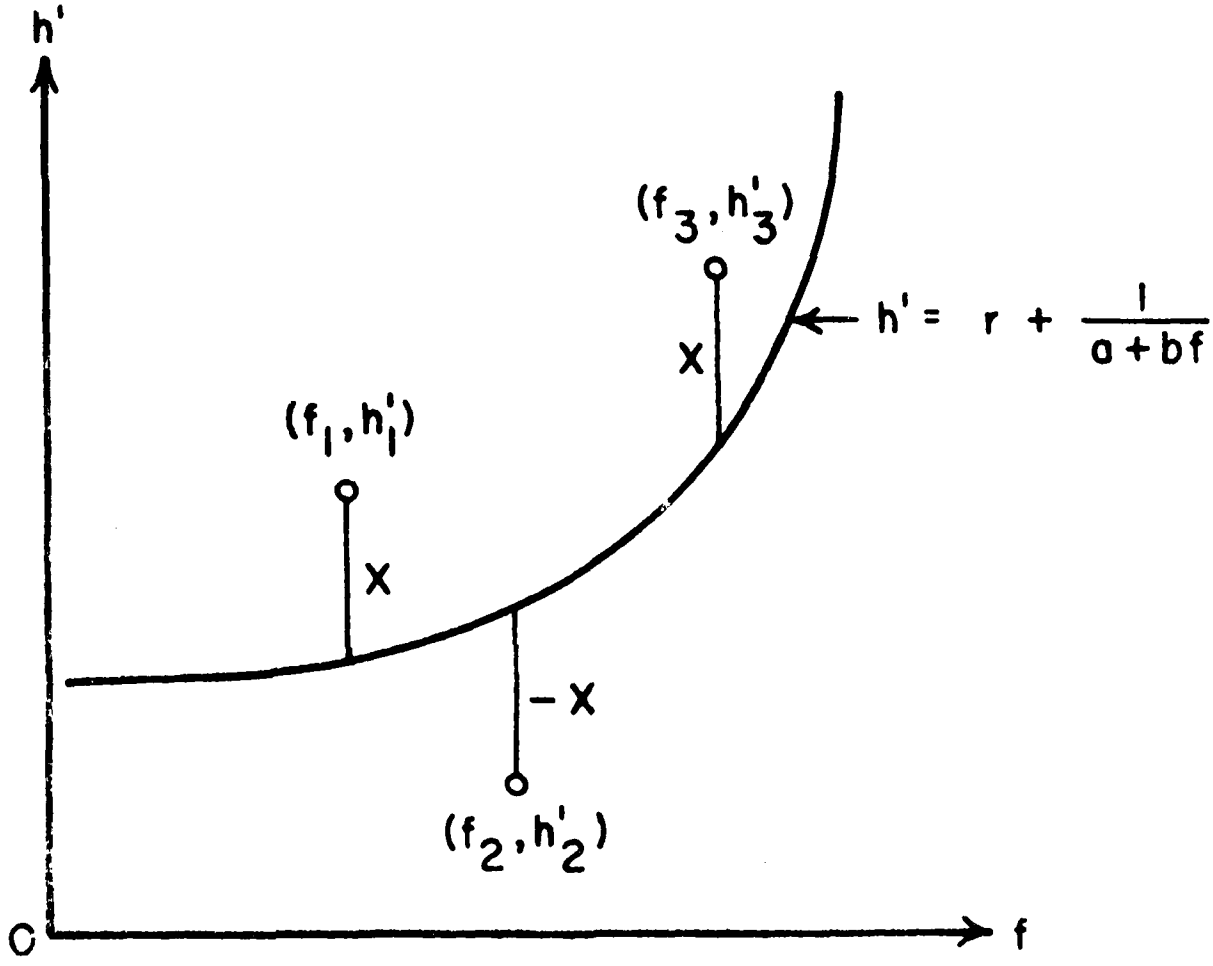

HYPERBOLIC FITTING WITH MIN-MAX METHOD

Figure 5

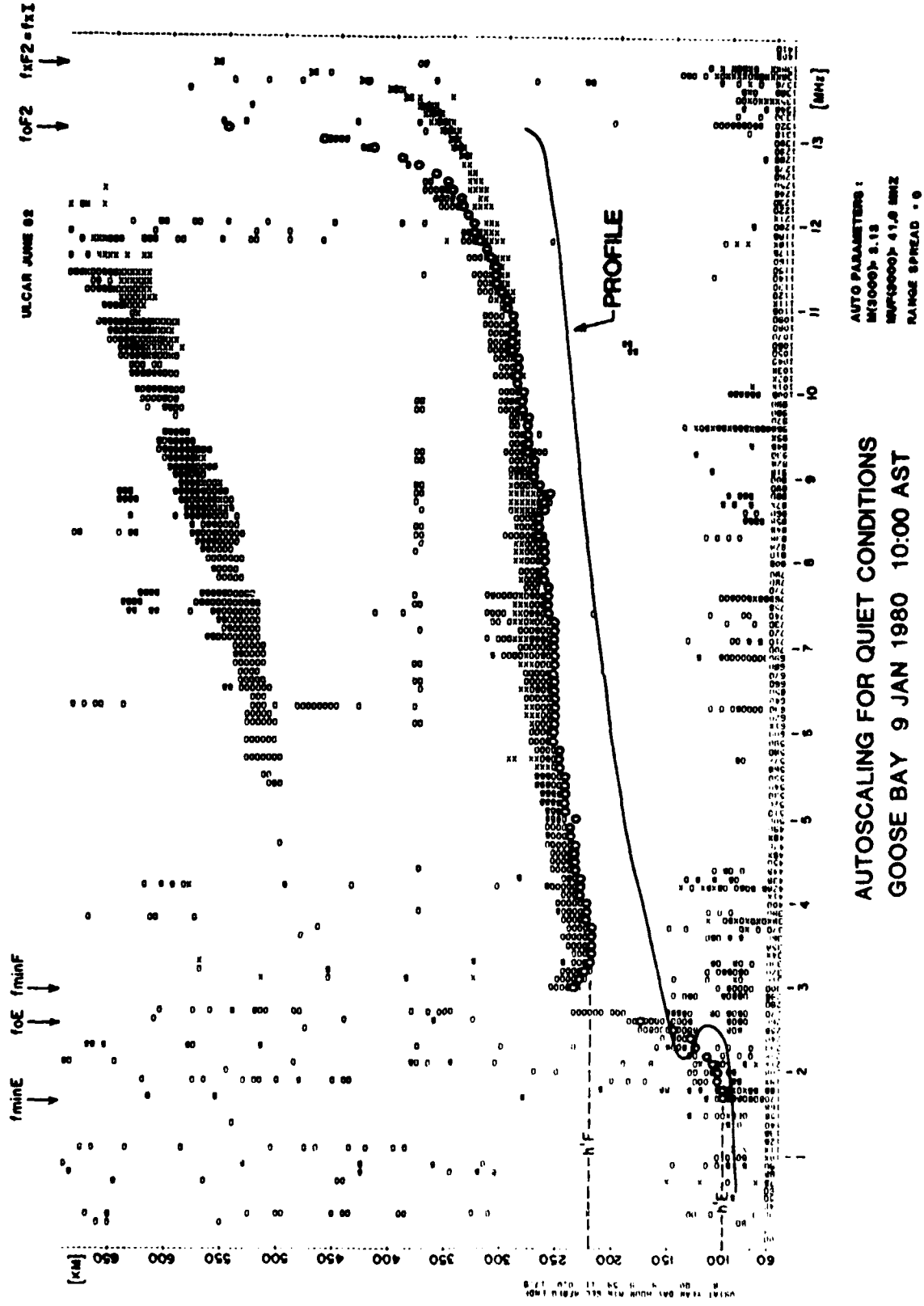
fxF2=fxI
foF2
fminE
foE
fminF
h'F
h'E
PROFILE
ULCAR JUNE 82
AUTOSCALING FOR QUIET CONDITIONS
GOOSE BAY 9 JAN 1980 10:00 AST
[MHz]
[km]

Figure 6

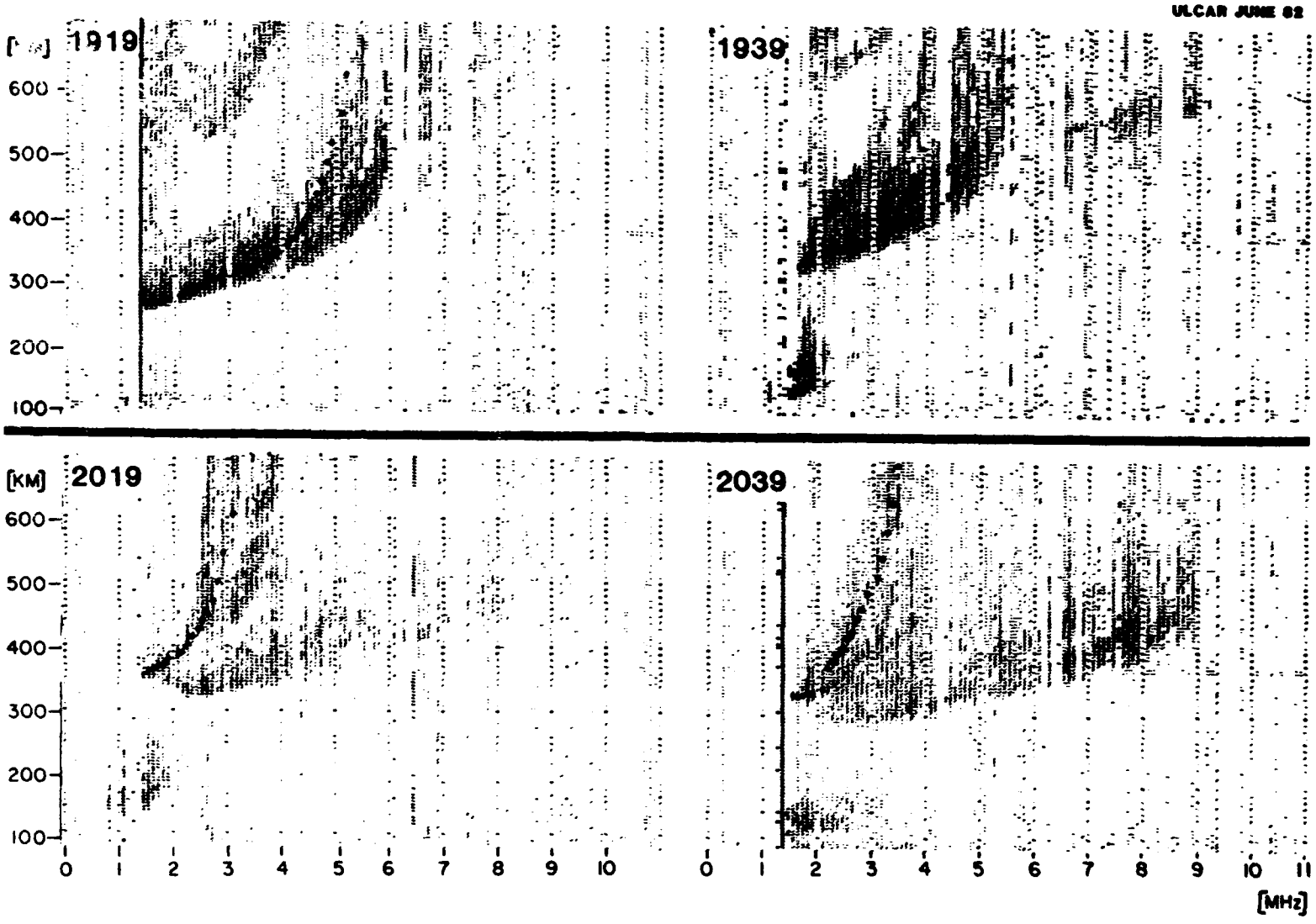

AUTOSCALING DURING TROUGH CONDITIONS

GOOSE BAY 7 JAN 1980

Figure 7

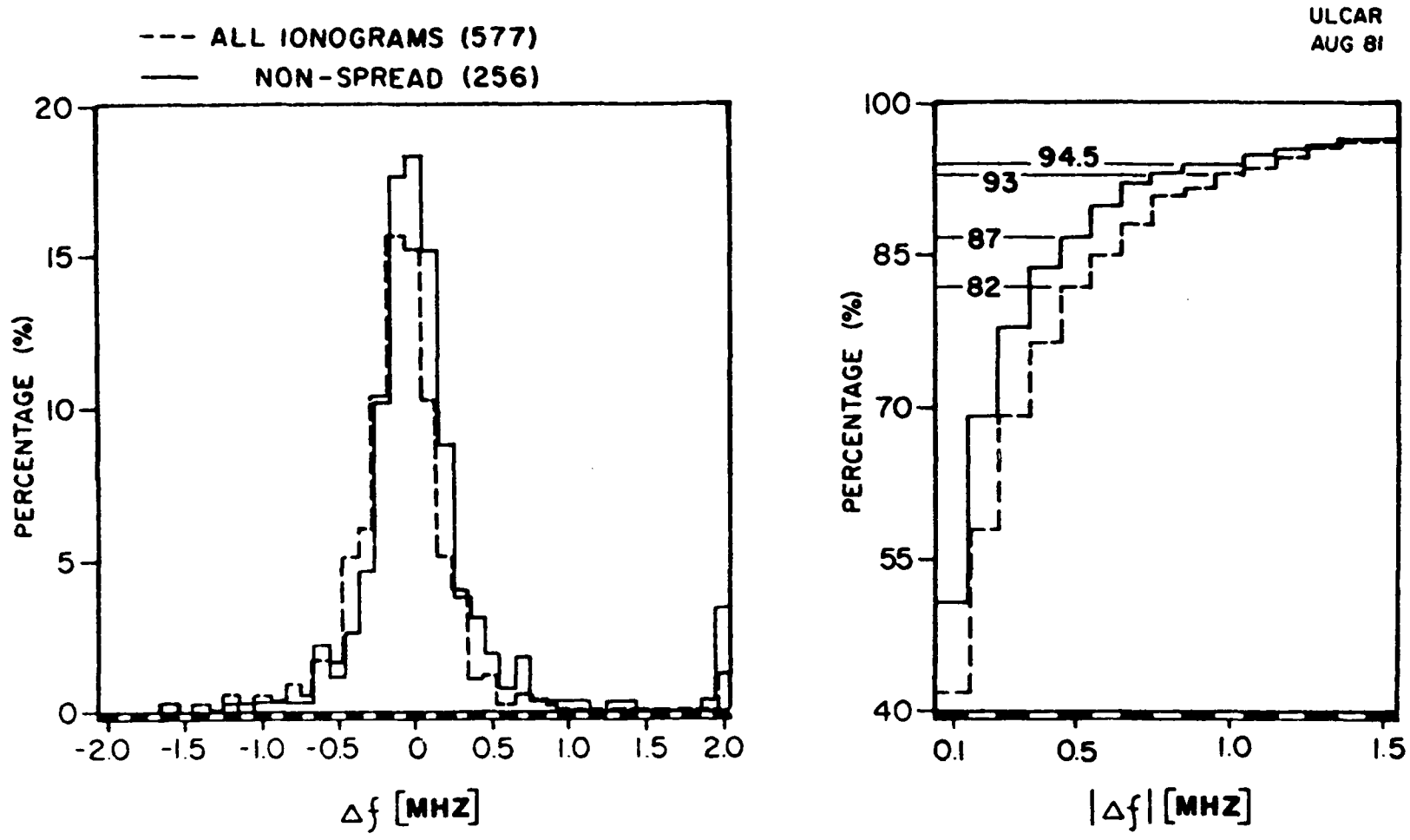

ERROR DISTRIBUTION OF FOF2 (MANUAL FOF2 - AUTO FOF2)
GOOSE BAY JANUARY 1980

Figure 8

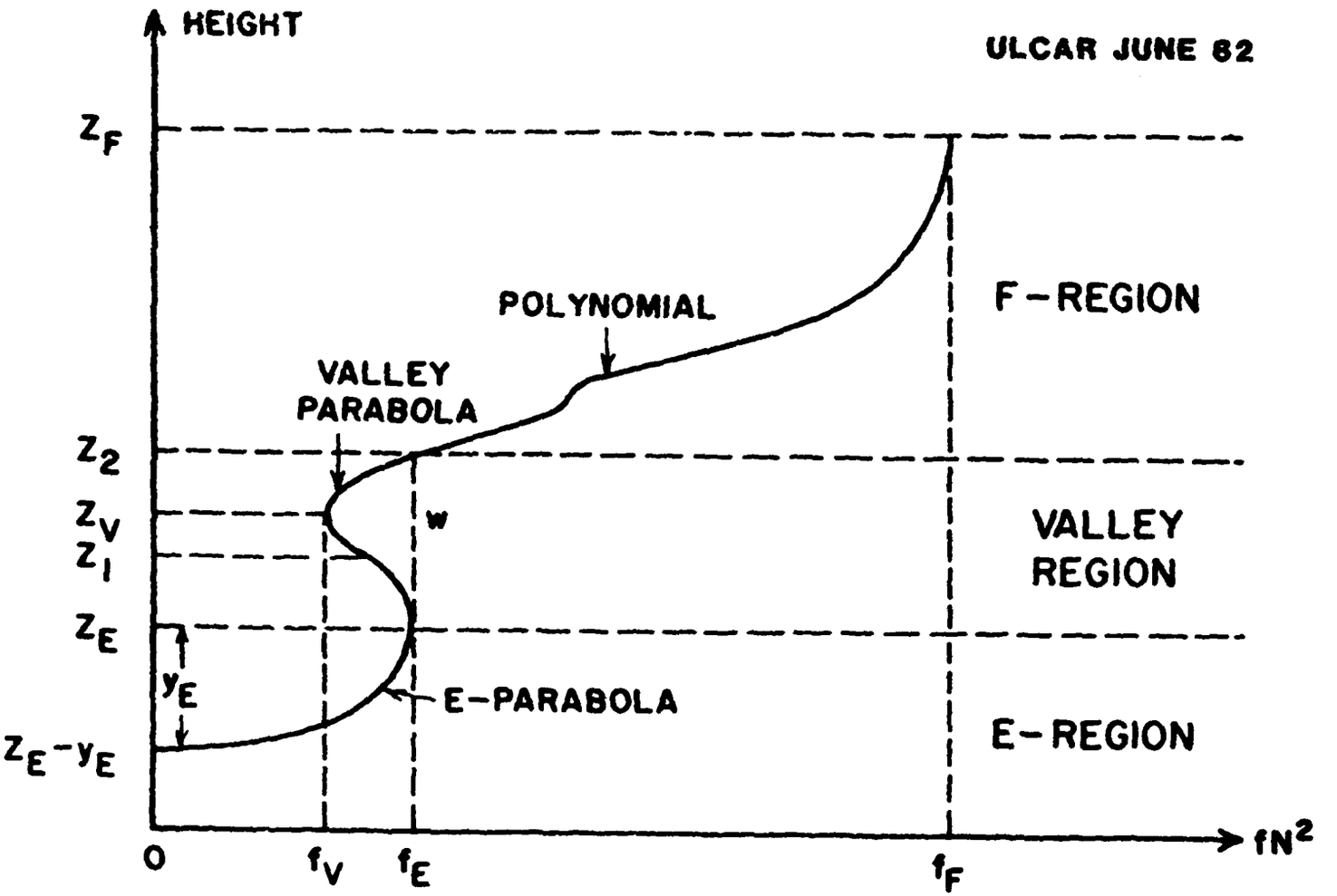

ELECTRON DENSITY PROFILE MODEL

Figure 9

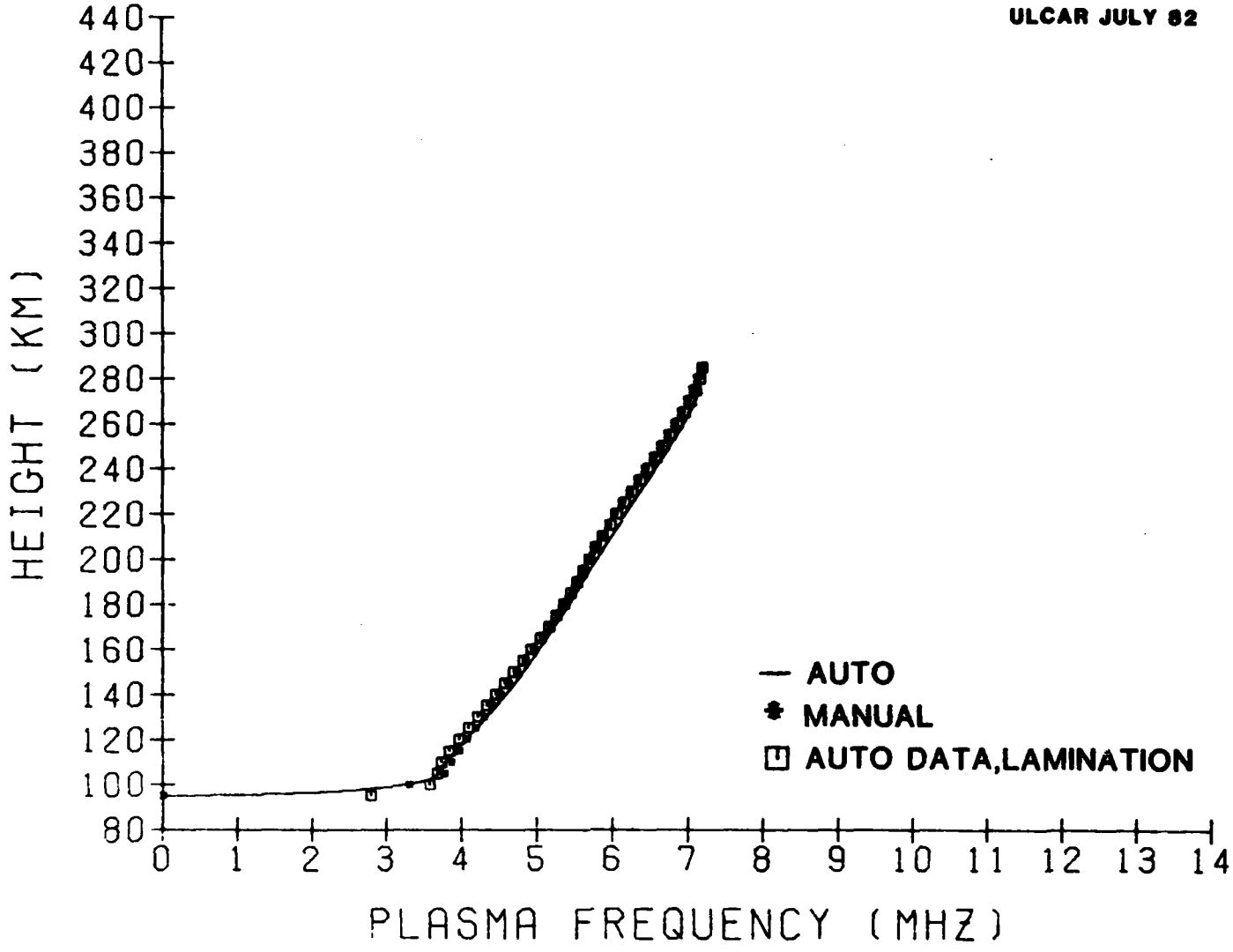

DAYTIME PROFILE for QUIET CONDITIONS

GOOSE BAY 21 APR. 1980, 10:00 AST.

Figure 10

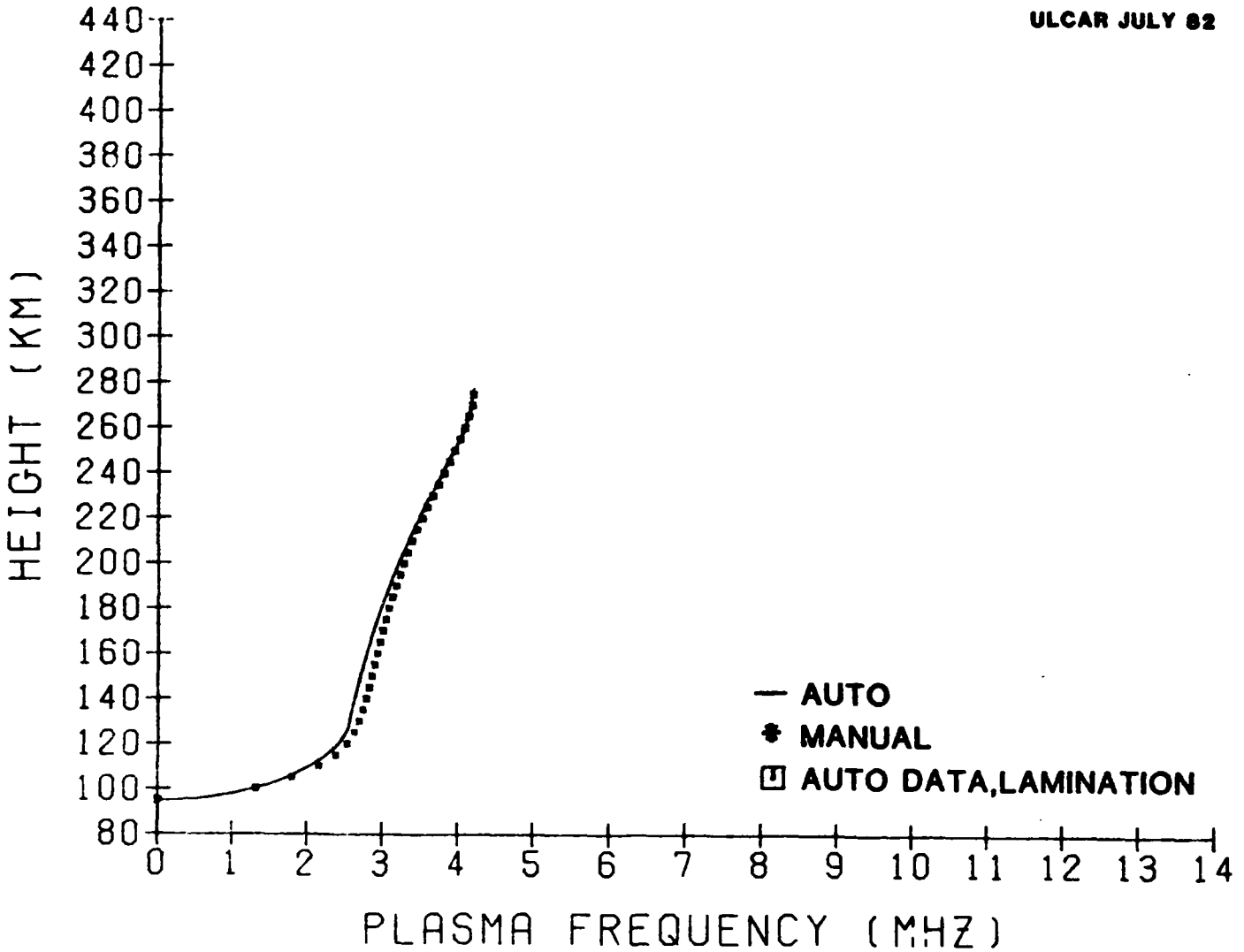

NIGHTTIME PROFILE during DISTURBED CONDITIONS

GOOSE BAY 5 SEP. 1980, 20:19 AST.

Figure 11

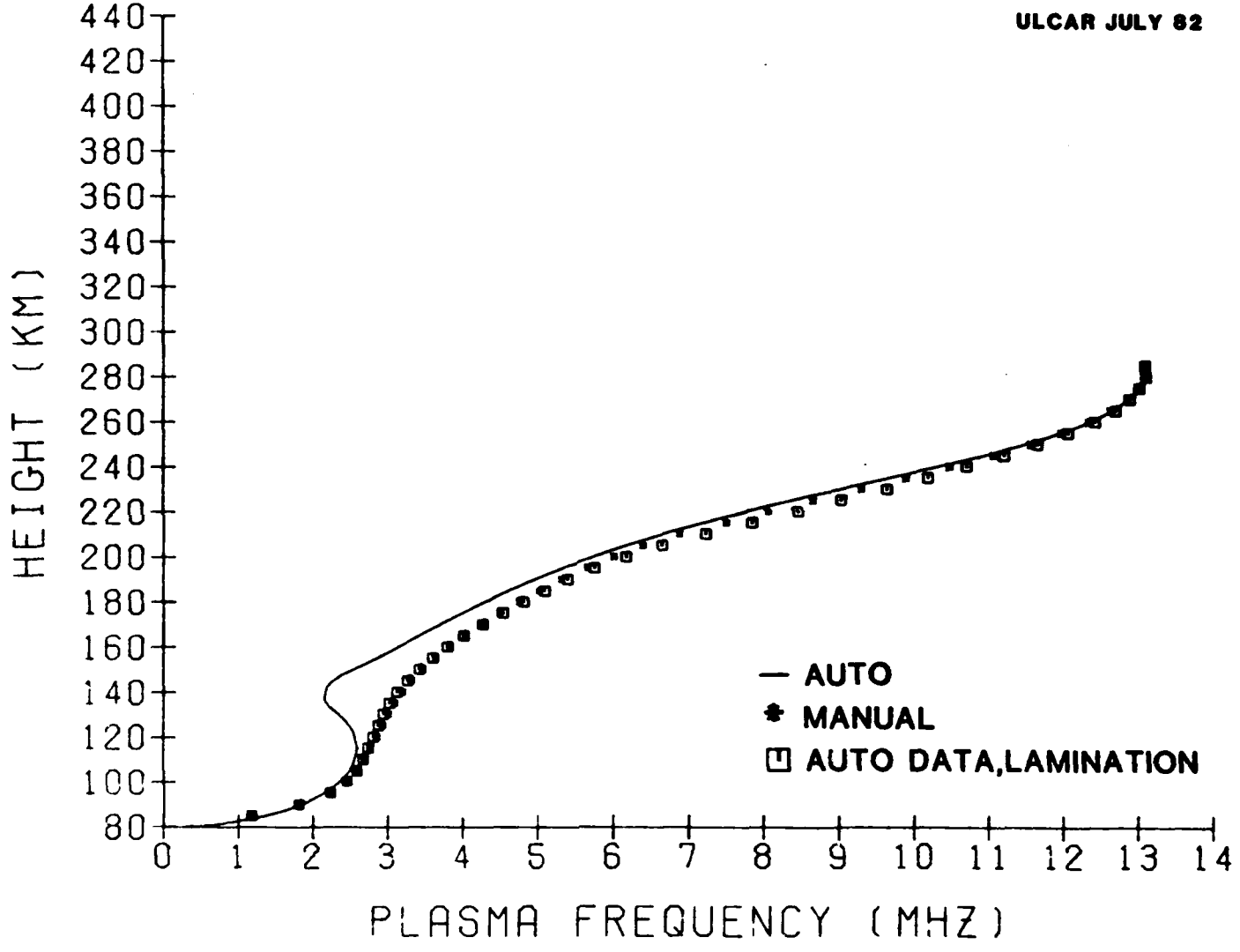

DAYTIME PROFILE with IONIZATION VALLEY

GOOSE BAY 9 JAN 1980, 10:00 AST.

Figure 12

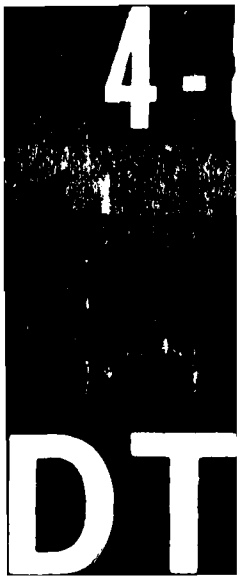
4-
DT